



PAPER 77-13

This document was produced
by scanning the original publication.

Ce document est le produit d'une
numérisation par balayage
de la publication originale.

**DIPOLE ELECTROMAGNETIC MAPPING
OF PERMAFROST TERRAINS:
THEORETICAL DEVELOPMENTS
AND COMPUTER PROGRAMS**

A.K. SINHA





**GEOLOGICAL SURVEY
PAPER 77-13**

**DIPOLE ELECTROMAGNETIC MAPPING
OF PERMAFROST TERRAINS:
THEORETICAL DEVELOPMENTS
AND COMPUTER PROGRAMS**

A.K. SINHA

1977

Minister of Supply and Services Canada 1977

Printing and Publishing
Supply and Services Canada,
Ottawa, Canada K1A 0S9,

from the Geological Survey of Canada
601 Booth St., Ottawa, K1A 0E8

or through your bookseller.

Catalogue No. M44/77-13
ISBN - 0-660-00836-X

Price: Canada: \$2.50
Other Countries: \$3.00

Price subject to change without notice

CONTENTS

	Page
Abstract/Résumé	1
Introduction	1
Theoretical considerations	3
Description of the Program	7
A. Main Program COMPUT	7
B. Subroutine SUBM	7
C. Subroutine EULER and Functions J0X, J1X and GG	9
Numerical results	9
Concluding remarks	13
References	14
Appendix	15

Illustrations

Figures 1	3
" 2-5	8
" 6-9	10
" 10-13	11
" 14-17	12

DIPOLE ELECTROMAGNETIC MAPPING OF PERMAFROST TERRAINS: THEORETICAL DEVELOPMENTS AND COMPUTER PROGRAMS

Abstract

Multifrequency electromagnetic mapping using dipolar sources may be useful for detecting and delineating permafrost in high latitude areas such as the arctic regions of Canada. A theoretical study has been made on the relative suitability of five coil arrangement systems for mapping permafrost where it occurs as the top layer of a two-layer medium, underlain by unfrozen sediments. The computer modeling study has indicated that the horizontal coplanar system would be the best from the viewpoint of the anomaly magnitude, while the perpendicular system might offer the highest resolution. The null-coupled, inclined, parallel system comes close in performance to the horizontal coplanar system.

The generalized computer program for obtaining the response of an n-layer lossy dielectric medium excited by harmonic dipolar sources has been included in the Appendix. The program is completely general and valid for any frequency, coil separation and electrical constants of the media. Hence, it may be used to generate theoretical response of any layered model necessary for the interpretation of multifrequency field data.

Résumé

Le levé cartographique électromagnétique à fréquence multiples effectué à partir de sources bipolaires peut servir à détecter et à délimiter les couches de pergélisol que l'on retrouve dans les zones de haute latitude, comme les régions arctiques du Canada. Une étude théorique a été entreprise quant aux avantages que pouvaient offrir les systèmes à cinq bobines pour effectuer le levé des couches de pergélisol, lorsqu'il constitue la couche supérieure d'un sous-sol formé lui-même de deux couches reposant sur des sédiments non gelés. L'étude du modèle sur ordinateur a indiqué que le système coplanaire horizontal permettait le mieux de mesurer l'importance de l'anomalie, alors que le système perpendiculaire quant à lui offrait la meilleure définition. Le système parallèle, incliné et à couplage nul offre presque les mêmes possibilités que le système coplanaire horizontal.

Le programme général sur ordinateur qui permet d'obtenir la réaction d'un corps amortisseur diélectrique de n couches soumis aux impulsions de sources bipolaires harmoniques figure à l'annexe. Le programme, de portée générale, est valable quelle que soit la fréquence, la séparation de la bobine et les constantes électriques des corps. On peut donc l'utiliser pour provoquer une réaction théorique d'un modèle disposé en couche lorsqu'il est nécessaire d'interpréter des données en plusieurs fréquences obtenues sur le terrain.

INTRODUCTION

Permafrost or permanently frozen ground is defined to be soil or rock material that has remained below 0°C continuously for more than two years (Ferrians and Hobson, 1973). It is present under vast stretches of land and sea at higher latitudes, such as the Arctic regions of Canada and Alaska. The presence of permafrost often coincides with the presence of ice, and this may significantly alter the physical properties of the terrain. During summer, the top part of the ground in a permafrost terrain may reach temperatures above 0°C causing melting of ice in the pore volumes. When the temperature returns to below 0°C in winter, the thawed ground freezes again. The layer which thaws and refreezes each year may be of variable thickness and is called the 'active' layer. Below the permafrost layer, which lies just below the active layer, the ground is usually unfrozen. Thus during summer, the permafrost terrain may be perceived as being a three-layer medium. During winter, however, when the active layer is frozen, only two distinct layers, the frozen top layer and the unfrozen layer may be distinguished.

The freezing of the ground results in two distinct changes in its physical properties. Firstly, it causes a significant increase in its electrical resistivity, and secondly, the seismic wave velocity through it increases. In electromagnetic exploration, we try to exploit the first type of change. It has been reported (Ananyan, 1958) that the ratio of the resistivity of frozen to unfrozen ground may range from 10 for fine grained materials to as much as 1000 for coarse grained rocks. Thus significant resistivity changes may be detected by electrical or electromagnetic methods. In most areas of northern Canada, the permafrost terrains are highly resistive and the contrast in resistivity between frozen and unfrozen ground ranges from moderate to high. In analytical studies, therefore the permafrost zones should be considered as lossy dielectrics.

The discovery in recent years of significant deposits of fossil fuels and minerals in Alaska and Northwest Territories, Canada, has led to an increased interest in the mapping of permafrost terrains of the north. Several geophysical methods, mainly electrical and electromagnetic techniques, have been tried for the purpose. D.C. resistivity surveys have been used widely in the past for permafrost mapping (MacKay, 1969). However, they suffer from two problems in permafrost regions, namely, high cost of operation and high contact resistance of the ground which makes surveying difficult. In recent years, therefore, non-contact or electromagnetic methods have been tried for this purpose. The Radiohm (Collett and Becker, 1968) method which uses VLF transmissions to measure the surface impedance of the ground has been found to be quite useful and is reported to be capable of mapping the ground to a resolution of 25m^2 (Hoekstra, et. al., 1975). The E-Phase technique, which uses several radio transmitters as sources, has been used by Barringer Research Ltd. for airborne mapping of permafrost terrains in the Northwest Territories, Canada. But it has been shown (Sinha, 1977a) that when the ground resistivities and frequencies are high, the effects of altitude of the aircraft and displacement currents on the observed results may be significant. Since these two factors are ignored in E-Phase interpretation, the interpreted resistivity values are likely to be erroneous over permafrost zones. Audio Frequency Magnetotelluric (AMT) methods (Koziar and Strangway, 1975) and radar methods (Annan and Davis, 1976) have also been used successfully over permafrost areas. Since the AMT method uses distant natural sources, its resolution is likely to be somewhat poor because a large volume of the ground is sampled. The radar method is quite accurate but its limitations are high cost and inability to see through the ground if any conducting layer like clay is present near the surface.

In this paper, we will discuss the possibility of using a multifrequency double-dipole e.m. system for permafrost mapping. Single frequency dipole-dipole systems have been used in mining geophysics and in mapping ground for geotechnical purposes for many years. It is only recently, however, that multifrequency e.m. dipole systems have become available. A technique for determining the resistivity and dielectric constant of a homogeneous permafrost terrain from multifrequency double-dipole sounding results was discussed earlier (Sinha, 1974, 1976a). Since in most areas permafrost is not homogeneous but layered, the case of a layered lossy dielectric excited by oscillating magnetic dipoles will be considered here. As permafrost regions are generally resistive, relatively high frequencies will have to be used in mapping them for adequate resolution. Hence displacement currents in air and in all the media will have to be considered.

In this paper the author has presented the complete solutions for the electromagnetic fields scattered by an n-layer lossy dielectric earth excited by oscillating magnetic dipoles for any frequency range. It is obvious however that when more than two layers are present, the number of possible parameters becomes rather large and any attempt to present master-charts for even a few typical cases would be futile. The only realistic thing to do in such a case is to present the computer program for the calculation of the mutual coupling ratios of loops in all systems so that anyone may obtain any desired theoretical curve for any set of data.

A generalized computer program has been written which provides the mutual coupling ratios of two loops over an n-layer lossy medium in all five coil configuration systems (Fig. 1) used by the industry. The program is valid for any frequency, coil separation or coil altitude and for any resistivity and dielectric constants of the layers. A similar program for the case when displacement currents are negligible was published previously (Sinha and Collett, 1973). The program along with some sample outputs for two- and three-layer lossy dielectric media are included in the Appendix. Since portability of an instrument is very important in Arctic terrains, a coil separation of 3 m and altitude of 1 m for the coils have been assumed in deriving the sample output. It is hoped that this computer program will be helpful in interpreting dipole e.m. sounding data over permafrost terrain.

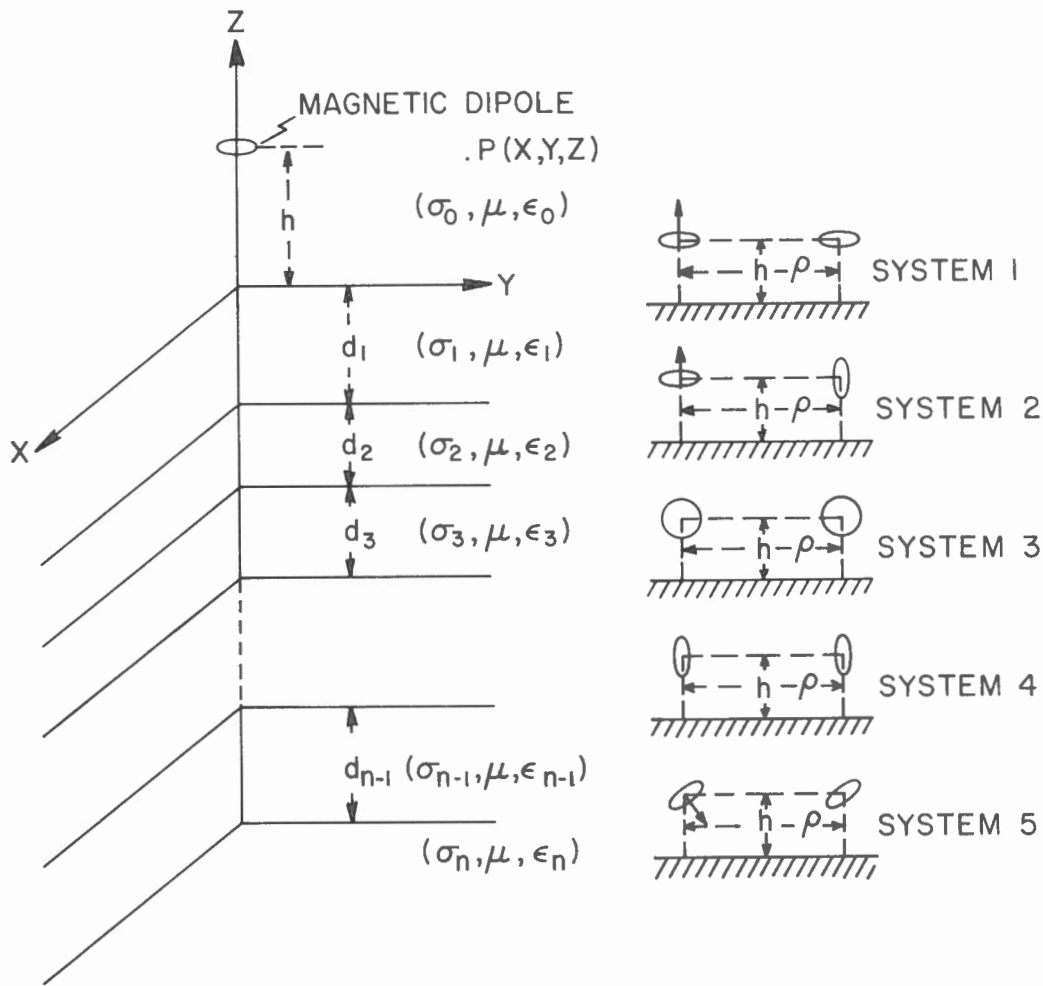


Figure 1. Magnetic dipole over n -layer earth and the five coil systems considered in the text.

THEORETICAL CONSIDERATIONS

Let us suppose that an arbitrarily oriented magnetic dipole carrying a harmonic current $I \exp(i\omega t)$ and of area dA is placed along the Z -axis of a rectangular co-ordinate system at a height h over an n -layer lossy dielectric earth (Fig. 1). The electrical constants of air are $(\sigma_0, \mu, \epsilon_0)$, σ_0 being infinitesimally small, and those of the layers being given by $(\sigma_m, \mu, \epsilon_m)$, where the subscript m varies from 1 to n . The point of observation is taken to be any point P over the earth with co-ordinates (x, y, z) in cartesian and (r, ϕ, z) in cylindrical system. The permeabilities of all the media are assumed to be identical, the same as that of a vacuum and designated by μ ($4\pi \times 10^{-7}$ H/m). The thicknesses of the layers are given by d_m where m varies from 1 to $(n-1)$. All the layers are assumed to be homogeneous and isotropic and all interfaces parallel to the air-earth boundary. International System (SI) of units are used throughout.

The arbitrarily oriented dipole may be split into two component dipoles, one horizontally and the other vertically directed. Assume that the strengths of the dipole components are the same and given by M . The electromagnetic field components in any medium may be defined in terms of a vector potential \vec{F} given by:

$$(1) \quad \vec{E} = -\text{Curl } \vec{F}$$

$$(2) \quad i\omega\mu \vec{H} = \text{grad div } \vec{F} - \gamma^2 \vec{F}$$

where γ is the propagation constant of the medium given by

$$(3) \quad \gamma = \left[i\omega\mu (\sigma + i\omega\epsilon) \right]^{1/2}$$

where ω is the angular frequency and $i = \sqrt{-1}$.

Considering the vertical dipole first, from symmetry it is clear that it will only have one secondary vector potential component F_{Zm} which will satisfy in all the media the Helmholtz equation

$$(4) \quad (\nabla^2 - \gamma_m^2) F_{Zm} = 0$$

where $m = 0, 1, 2, \dots, n$

Hence the vector potential F_{Z0} at $P(r, \phi, z)$ is given by (Sinha, 1976a)

$$(5) \quad F_{Z0} = \frac{IdA i\omega\mu}{4r} \int_0^\infty \left[\frac{\lambda}{u_0} e^{-u_0 |z-h|} + \frac{\lambda}{u_0} R_{TE}(\lambda) e^{-u_0(z+h)} \right] J_0(\lambda r) d\lambda$$

where the first term is the source effect and the second term, due to the secondary field effects. $J_0(\lambda r)$ is a Bessel function of order zero and λ is the variable of integration. In the above equation

$$(6) \quad u_0 = (\lambda^2 + \gamma_0^2)^{1/2}, \quad \text{where } \gamma_0^2 = -\omega^2 \mu \epsilon_0$$

$R_{TE}(\lambda)$ is the reflection coefficient for the transverse electric (TE) mode and its value in terms of the constants of the media are known (Wait, 1966; Sinha, 1976a). Considering the Y-directed horizontal magnetic dipole component of moment M at the same location, the vector potential at $P(r, \phi, z)$ may be written as (Dey and Ward, 1970; Sinha, 1976a).

$$(7) \quad F_{Y0} = \frac{IdA i\omega\mu}{4\pi} \int_0^\infty \left[\frac{\lambda}{u_0} e^{-u_0 |z-h|} + \frac{\lambda}{u_0} R_{TM}(\lambda) e^{-u_0(z+h)} \right] J_0(\lambda r) d\lambda$$

$$(8) \quad F_{Z0} = -\frac{IdA i\omega\mu \cos \phi}{4\pi} \int_0^\infty \left[R_{TM}(\lambda) + R_{TE}(\lambda) \right] J_1(\lambda r) d\lambda$$

where $R_{TM}(\lambda)$ is the reflection coefficient for the transverse magnetic mode (TM) and has been expressed in terms of the parameters of the media (Sinha, 1976a).

From equations (2), (5), (7) and (8), the expressions for the magnetic field components H_x , H_y and H_z at P due to both vertical and horizontal dipoles may be written in terms of known parameters. If h_1 and h_2 are the altitudes of the transmitter and the receiver coils and 'r' their horizontal separation, the secondary field components at $P(x, y, z)$ may be written down as

Vertical Magnetic Dipole:

$$(9) \quad H_{x,s} = \frac{IdA}{4\pi \delta_1^3} T_3(A, B, D_j, k_j, e_j) \left(\frac{x}{r} \right)$$

$$(10) \quad H_{y,s} = \frac{IdA}{4\pi \delta_1^3} T_3(A, B, D_j, k_j, e_j) \left(\frac{y}{r} \right)$$

$$(11) \quad H_{z,s} = \frac{IdA}{4\pi \delta_1^3} T_0(A, B, D_j, k_j, e_j)$$

Y-Directed Horizontal Dipole:

$$(12) \quad H_{x,s} = \frac{IdA}{4\pi \delta_1^3} \left[\left(\frac{xy}{r^2} \right) \left\{ T_2(A, B, D_j, k_j, e_j) + T_1(A, B, D_j, k_j, e_j) \right\} - \frac{1}{B} \left(\frac{2xy}{r^2} \right) \left\{ T_4(A, B, D_j, k_j, e_j) + T_5(A, B, D_j, k_j, e_j) \right\} \right]$$

$$(13) \quad H_{y,s} = \frac{IdA}{4\pi\delta_1^3} \left[\left(\frac{y^2}{r^2} \right) T_1 (A, B, D_j, k_j, e_j) - \left(1 - \frac{y^2}{r^2} \right) T_2 (A, B, D_j, k_j, e_j) + \frac{1}{B} \left(1 - \frac{2y^2}{r^2} \right) \left\{ T_4 (A, B, D_j, k_j, e_j) + T_5 (A, B, D_j, k_j, e_j) \right\} \right]$$

$$(14) \quad H_{z,s} = -\frac{IdA}{4\pi\delta_1^3} \left[\left(\frac{y}{r} \right) T_3 (A, B, D_j, k_j, e_j) \right]$$

where T_0, T_1, \dots, T_5 are six infinite integrals given by

$$(15) \quad T_0(A, B, D_j, k_j, e_j) = \int_0^\infty \frac{g^3}{\sqrt{g^2+R}} \cdot e^{-A\sqrt{g^2+R}} R_{TE}(g) J_0(gB) dg$$

$$(16) \quad T_1(A, B, D_j, k_j, e_j) = \int_0^\infty g \sqrt{g^2+R} e^{-A\sqrt{g^2+R}} R_{TE}(g) J_0(gB) dg$$

$$(17) \quad T_2(A, B, D_j, k_j, e_j) = \int_0^\infty \frac{Rg}{\sqrt{g^2+R}} \cdot e^{-A\sqrt{g^2+R}} R_{TM}(g) J_0(gB) dg$$

$$(18) \quad T_3(A, B, D_j, k_j, e_j) = \int_0^\infty g^2 e^{-A\sqrt{g^2+R}} R_{TE}(g) J_1(gB) dg$$

$$(19) \quad T_4(A, B, D_j, k_j, e_j) = \int_0^\infty \frac{R}{\sqrt{g^2+R}} \cdot e^{-A\sqrt{g^2+R}} R_{TM}(g) J_1(gB) dg$$

$$(20) \quad T_5(A, B, D_j, k_j, e_j) = \int_0^\infty \sqrt{g^2+R} \cdot e^{-A\sqrt{g^2+R}} R_{TE}(g) J_1(gB) dg$$

The fields due to an inclined dipole (System 5) may easily be determined from field values for horizontal and vertical dipoles. In the above formulae

$$(21) \quad A = (h_1 + h_2)/\delta_1, \quad B = r/\delta_1, \quad D_j = 2d_j/\delta_1$$

where $j = 1, 2, \dots, (n-1)$

$$(22) \quad k_j = \sigma_j/\sigma_1 \quad \text{and} \quad e_j = \epsilon_j/\epsilon_0$$

where $j = 1, 2, \dots, n$

$$(23) \quad R = \frac{2}{\epsilon_1(1 - \sqrt{1+P^2})}, \quad P = \sigma_1/\omega\epsilon_1$$

$$(24) \quad \delta_1 = \text{Skin depth in the top layer} = \left\{ \frac{2}{\omega^2 \mu \epsilon_1 (\sqrt{1+P^2} - 1)} \right\}^{1/2}$$

In the special case when the frequency and resistivity of the ground is low (quasi-static case), the above generalized formulas reduce to the quasi-static formulas given earlier (Sinha and Collett, 1973). Thus, when P is large, $R \rightarrow 0$. Then integrals T_2 and T_4 reduce to zero and T_0 and T_1 become identical. Since it is customary to measure the mutual coupling of loops rather than the fields, the results will now be written in terms of the mutual coupling ratio values in five coil systems, mostly in use.

The mutual impedance Z between two coils is given by

$$(25) \quad Z = - \frac{i\omega\mu dA.N.H}{I}$$

where dA and N refer to the area and the number of turns of the receiver loop. H and I refer to the magnetic field along the axis of the receiver loop and the current in the transmitter loop respectively. Since the mutual coupling Z_0 between two coplanar and two coaxial loops in air are known (Sinha, 1976a), these values may be used as the normalizing factors to eliminate the areas and the number of turns of the coils from the final expression. Thus the mutual coupling ratio (Z/Z_0) in the five coil systems may be written down as

System 1. Horizontal Coplanar Loops

$$(26) \quad Z/Z_0 = 1 - \frac{B^3 T_0(A, B, D_j, k_j, e_j) \cdot e^{\gamma_0 r}}{(1 + \gamma_0 r + \gamma_0^2 r^2)}$$

System 2. Perpendicular Loops

$$(27) \quad Z/Z_0 = - \frac{B^3 T_3(A, B, D_j, k_j, e_j) \cdot e^{\gamma_0 r}}{(1 + \gamma_0 r + \gamma_0^2 r^2)}$$

System 3. Vertical Coplanar Loops

$$(28) \quad Z/Z_0 = 1 - B^2 \left[T_4(A, B, D_j, k_j, e_j) + T_5(A, B, D_j, k_j, e_j) - BT_2(A, B, D_j, k_j, e_j) \right] \frac{e^{\gamma_0 r}}{(1 + \gamma_0 r + \gamma_0^2 r^2)}$$

System 4. Vertical Coaxial Loops

$$(29) \quad Z/Z_0 = 1 - \frac{B^2}{2} \left[T_4(A, B, D_j, k_j, e_j) + T_5(A, B, D_j, k_j, e_j) - B \cdot T_1(A, B, D_j, k_j, e_j) \right] \frac{e^{\gamma_0 r}}{(1 + \gamma_0 r)}$$

System 5. Inclined Parallel Loops

$$(30) \quad Z/Z_0 = \frac{B^2}{3} \left[T_4(A, B, D_j, k_j, e_j) + T_5(A, B, D_j, k_j, e_j) - B \{ 2T_0(A, B, D_j, k_j, e_j) + T_1(A, B, D_j, k_j, e_j) \} \right] \frac{e^{\gamma_0 r}}{(1 + \gamma_0 r + \gamma_0^2 r^2)}$$

It should be noted that System 5, where the axes of the loops are inclined at an angle of 54.7 degrees to the vertical is a null-coupled system. The Z_0 values for Systems 2 and 5 have been taken to be the same as that for the horizontal coplanar system. The integrals $T_0, T_1 \dots T_5$ are evaluated by the Gaussian Quadrature technique. Since the integrals contain Bessel functions $J_0(x)$ and $J_1(x)$ which are oscillatory, the integrals themselves become oscillatory. Hence the contribution of different segments are determined separately and their algebraic sum provides the value of the integral. Thus an integral may be written as a summation (Abramowitz and Stegun, 1965) like the following:

$$(31) \quad \int \psi(A, B, D, k, e) J_m(gB) dg = \sum_{j=1}^{\infty} \frac{(x_j - x_{j-1})}{2} \sum_{p=1}^n w_p \left\{ \psi_j(A, B, D, k, e) J_m(gB) \right\}_p + R_n$$

where x_j values are the zeros of the Bessel function $J_m(gB)$, R_n is the remainder, and $\{\psi_j(A, B, D, k, e)J_m(gB)\}_p$ is that function evaluated at g_p given by

$$(32) \quad g_p = \frac{1}{2} \left\{ (x_j - x_{j-1})x_p + (x_j + x_{j-1}) \right\}$$

where w_p and x_p are the weight factors and the abscissas of the Gaussian integration with n points.

Since the inclusion of displacement currents makes the integrals more oscillatory, 96 point Gaussian formula (i.e. a finer mesh) was used instead of the usual 32 or 48 point formulas used for quasi-static cases (Sinha and Collett, 1973). This, along with using 44 segments of the integral yielded accuracies of 1 ppm or better. In the low frequency range (negligible displacement currents) the computed values agreed very well with previously published results for the quasi-static case by Frischknecht (1967) and Sinha (1973).

DESCRIPTION OF THE PROGRAM

A. Main Program COMPUT

The main program COMPUT presented in the Appendix is used to calculate the real and imaginary parts of the mutual coupling ratio (Z/Z_0) between two loops over an n -layered lossy dielectric medium in the five coil systems described in Figure 1. From those values, the amplitude and phase (degrees) values are also obtained for any number of layers, any frequency, coil separation and coil elevation and any resistivity and dielectric constants of the layers. The program is effective when the coil elevation h is finite and breaks down when the coils are on the surface ($h = 0$). The program is written in Fortran IV for use in CDC CYBER 74 Computer available at the Department of Energy, Mines and Resources. However, it may be run on any other computer system with minor modifications.

In the program, 15 predefined frequency values from 1 Khz to 1 Mhz are selected at which the mutual coupling ratios are computed. The values are indicated in the array XX which may however be changed to suit the user. Further inputs specifying the number of layers (NUM), coil separation (RH), conductivity of the top layer (S_1) and the conductivity ratio values ($K(J)$) beginning with the bottom layer (σ_n/σ_1) are given in Card No. 70. The thicknesses and the dielectric constants of the layers beginning with the bottom layer are specified in the next two cards. A statement (Card 76) immediately following the input card is used to terminate the program after the desired computations have been made. The altitude of the coils H which is assumed to be the same for both transmitter and receiver coils is specified in Card No. 101. The DO loop beginning in Card No. 102 considers all the specified frequencies one by one. From the initial inputs and the frequency, the skin depth δ_1 in the top layer (DEL) and a parameter $CS (\omega \mu \delta_1)$ are computed which will be needed in the subroutine SUBM for computing the integrals. TEE is an integer which specifies the subscript n of the integral T_n being computed. OPT is an integer which may be 0 or 1 indicating whether the TE or the TM mode is being considered in computing the integral. The six integrals T_0, T_1, \dots, T_5 are evaluated at each frequency and their complex values are stored in six arrays R_1, R_2, \dots, R_6 . The complex mutual coupling ratios in the five systems are stored in arrays Q_1, Q_2, \dots, Q_5 respectively (cards 173-177). Finally, the real and the imaginary parts of (Z/Z_0) in the five systems (RA1, RA2, --- RA5 and AIM1, AIM2, --- AIM5) are computed as also the amplitude and phase values (degrees). After all the frequencies have been considered, the final results are printed out (cards 217-230). Sample outputs for the response of a two-layer and a three-layer permafrost medium excited by dipolar sources in five coil systems are presented at the end of the listings for two coil separation values.

B. Subroutine SUBM

This subroutine is called from the main program six times for the evaluation of the real and the imaginary parts of the infinite integrals T_0, T_1, \dots, T_5 . Subroutine SUBM has some similarity with subroutine CALC which was published earlier (Sinha and Collett, 1973) for obtaining infinite integrals for the quasi-static case. The data inputs for the parameters AW, W, XO, X1 are provided in the beginning of the subroutine. AW and W values (cards 81 and 82) indicate the abscissas (zeros of Legendre's polynomials) and the weight factors for the Gaussian integration respectively. In the generalized case under consideration, the integrals may oscillate quite fast which calls for a finer mesh for evaluating them. In the subroutine the 96 point formula is used which means that the areas between successive zeros of the Bessel functions are subdivided into 96 parts. Hence AW and W have 96 values each. XO and X1 indicate the positions of the zeros of the Bessel functions $J_0(X)$ and $J_1(X)$ respectively. In the subroutine, XO and X1 have 44 values each. The Z values (cards 116 and 120) correspond to the 'g' values in the integrals. At each value of AW, the value of g_p is determined from the function GG (card 135). A decision is made depending on the value of OPT (card 150) whether to consider the reflection coefficient for the TE or the TM mode, i.e., whether RTE or RTM

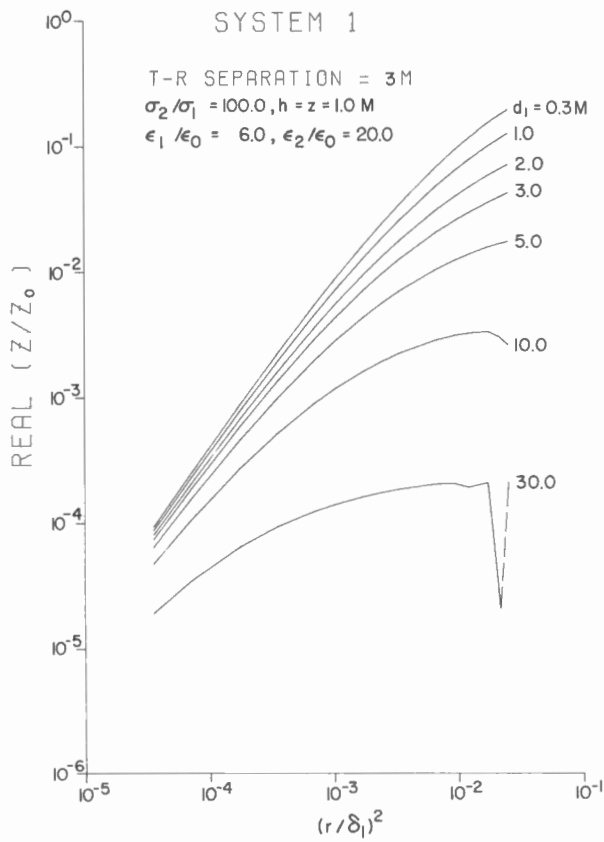


Figure 2. Plot of the real part of (Z/Z_0) versus $(r/\delta_1)^2$ for System 1 for several two layer models for a coil separation of 3 m.

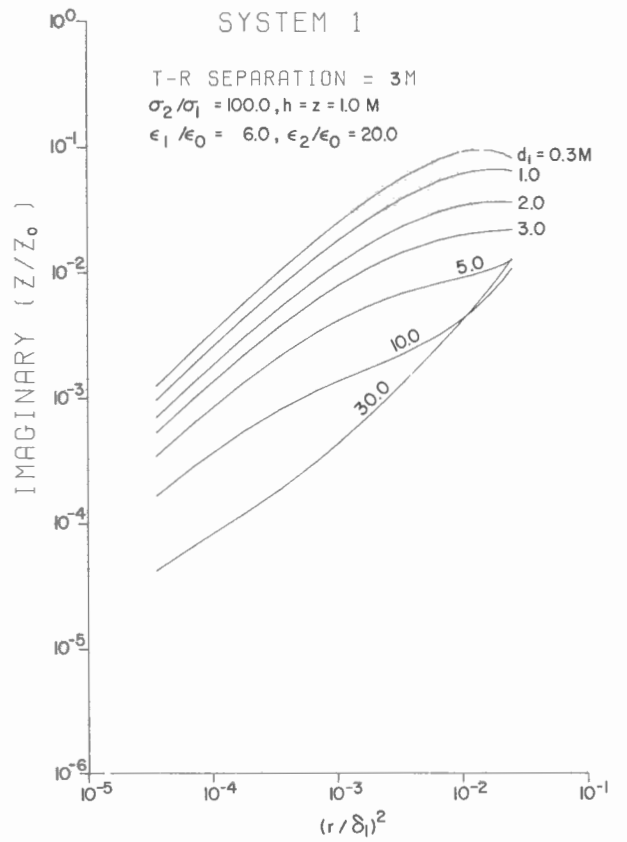


Figure 3. Plot of the imaginary part of (Z/Z_0) versus $(r/\delta_1)^2$ for System 1 for several two layer models for a coil separation of 3 m.

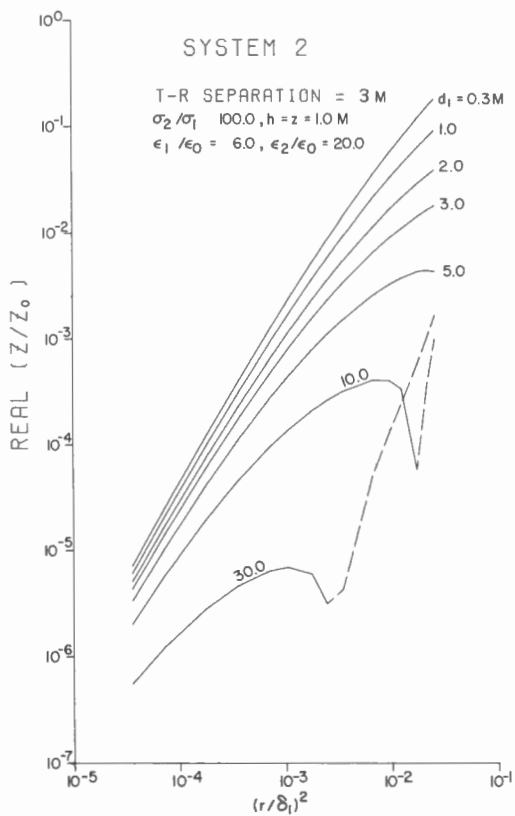


Figure 4. Plot of the real (Z/Z_0) versus $(r/\delta_1)^2$ for several two layer models for System 2 and a coil separation of 3 m.

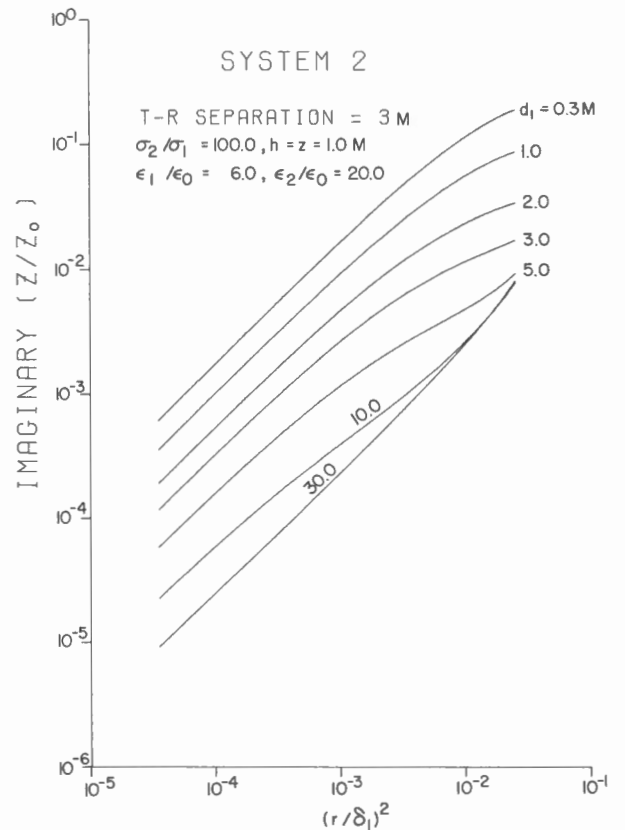


Figure 5. Plot of the imaginary (Z/Z_0) versus $(r/\delta_1)^2$ for several two layer models for System 2 and a coil separation of 3 m.

is to be determined. Once the reflection coefficients RFI (cards 194 or 197) or RG1 (cards 244 or 247) are obtained, and depending on the value of TEE, the function JWEX for that particular AW is computed. The algebraic sum of the JWEX or its real and imaginary parts for all 96 values provide the contribution to T_n over one segment bounded by two consecutive zeros of the Bessel function J_n . The values for all subsequent segments are stored in memory and used in subsequent tests for the convergence of the series. The test involves the calculation of the absolute ratio of the contribution from one segment to that of the first segment. Since the integrals are attenuated exponentially, the fall off in their values is quite rapid. In this program, when the ratio falls below 10^{-8} , the computation stops and the algebraic sum of all the contributions from all segments up to that point provide the value of the integral. Sometimes, when the height of the coils is small, the integrals may not converge quickly. If the convergence does not take place by the 44th segment, Euler's transformation (Abramowitz and Stegun, 1965) is used to obtain the sum of the series from the 22nd to the 44th segment. The sum is added to the previously computed algebraic sum of the first 21 segments to obtain the value of the integral. By using a small cut-off value of 10^{-8} and 96 point Gaussian formula, accuracies of 1 ppm or better are realized in most cases.

C. Subroutine EULER and Functions JOX, JIX and GG

Subroutine EULER is called from the subroutine SUBM twice when the convergence of the integrals is slow, i.e., when the ratio of the 44th to the first segment is greater than 10^{-8} , the cut-off value. The subroutine then sums up the contribution of the 22nd to the 44th segment by applying Euler's transformation. The outputs of the subroutine are EUSUR and EUSUI for the real and the imaginary parts of the contribution.

The function JOX computes the Bessel function of order zero for any argument X. There are two paths in the program. If the argument is less than 3, the series solution is used, while for larger values of argument, the polynomial solution is used. The function JIX computes the Bessel function of the order 1 for any argument using either the series or the polynomial approach. The function GG computes the function g_p defined in eqn. 32). The convergence of the integrals is controlled largely by the value of $A(2h/\delta_1)$ since it occurs as $\exp(-A\sqrt{g^2 + R})$. If the coils are placed on the surface ($h = 0$), the integrals become divergent.

NUMERICAL RESULTS

The theoretical results and the accompanying computer program in the Appendix have been used to obtain some numerical results on the variation of the mutual coupling ratio (Z/Z_0) between two loops over a two-layer lossy dielectric model simulating permafrost conditions. A similar study for the case of a homogeneous lossy dielectric was published earlier (Sinha, 1976a) with the twin aim of determining the best coil system for permafrost exploration and to find out a method of interpreting the data. Since permafrost terrains are, in general, not homogeneous it is more realistic to deal with plane-layered models although even that might be an approximation in the case of discontinuous permafrost zones. In summer, the presence of the conductive active layer at the top precludes the use of multifrequency e.m. (with frequencies going up to 1 Mhz) methods since most of the energy will be absorbed in that layer. During winter, when the active layer is frozen, we have the typical two-layer situation with the frozen layer at the top underlain by the unfrozen sediments. Since the resistive frozen layer will transmit the incident energy without much attenuation, multifrequency e.m. exploration for permafrost will be ideal during winter.

As logistics are difficult in the arctic, any instrument to be useful there should be very portable, i.e., capable of being carried by one or two persons. In the theoretical simulations, therefore, coil separations of 2 and 3 m and coil elevations of 1 m above the ground have been considered. Since permafrost resistivities vary widely, frequencies from 1 Khz to 1 Mhz, i.e., a spread of three decades, have been considered for sufficient resolution and depth penetration.

In the first set of computations, the coil separation was taken to be 3 m, conductivity σ_1 and the conductivity contrast σ_2/σ_1 were taken to be 0.001 S/m and 100.0 respectively. The dielectric constants of the frozen and the unfrozen layers were assumed to be 6.0 and 20.0. Seven values of the thickness d_1 of the top layer were considered. Figures 2 and 3 illustrate the variation of the real and imaginary parts of (Z/Z_0) against the non-dimensional parameter $(r/\delta_1)^2$ for System 1, where, as before r and δ_1 are the coil separation and skin depth in the top layer. The dashed sections represent values that have been reversed in sign for plotting purposes.

In Figures 2 and 3, at low frequencies (low r/δ_1) and small d_1 values, the bottom layer influence is predominant. As the frequency is increased, the skin depth decreases and the top layer influence grows. The curve therefore, turns and tends to follow a curve which represents the effect of the top layer only. When both frequency and d_1 are large, the currents are almost exclusively confined in the top layer and the response is close to that of a homogeneous dielectric, i.e., as if the bottom layer did not exist. At intermediate values of d_1 , the response shifts from the curve for $d_1 \rightarrow 0$ to the case of $d_1 \rightarrow \infty$ as the frequency is increased. The curves of Figure 3 appear to be quasi-parallel but are, in fact, distinguishable by different slopes. The resolutions of the curves are also adequate except when the frequency and thickness d_1 are large ($d_1 > 10$ m).

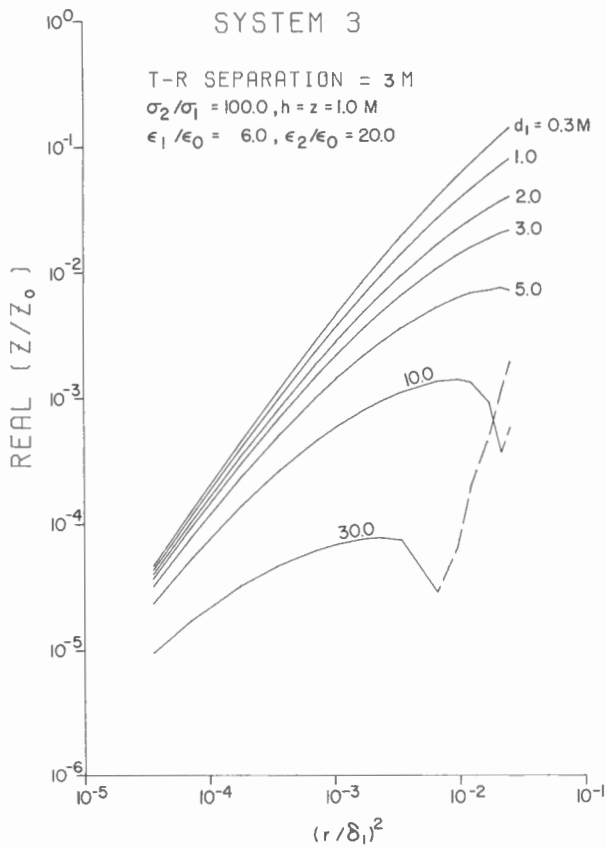


Figure 6. Variation of real (Z/Z_0) against $(r/\delta_1)^2$ for a coil separation of 3 m over several two layer models for System 3.

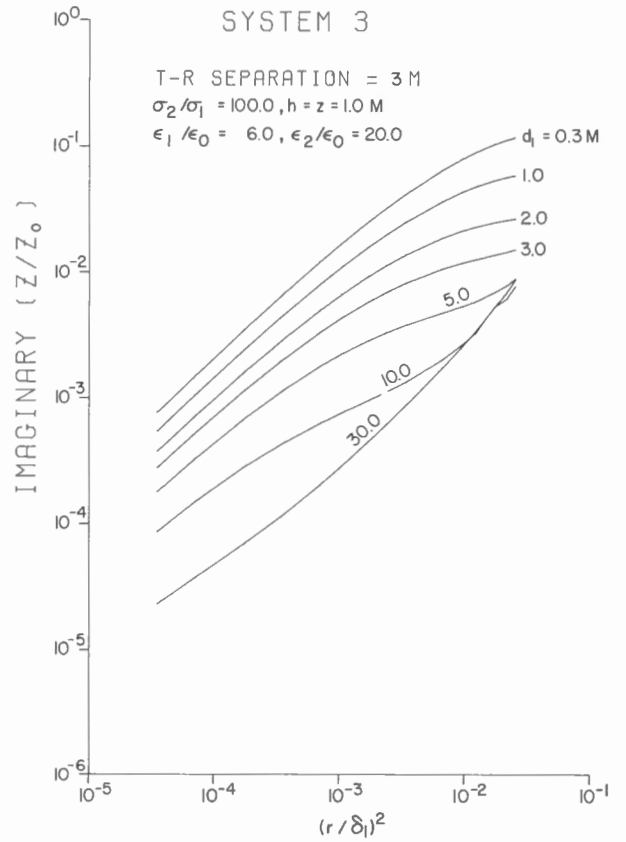


Figure 7. Variation of imaginary (Z/Z_0) against $(r/\delta_1)^2$ for a coil separation of 3 m over several two layer models for System 3.

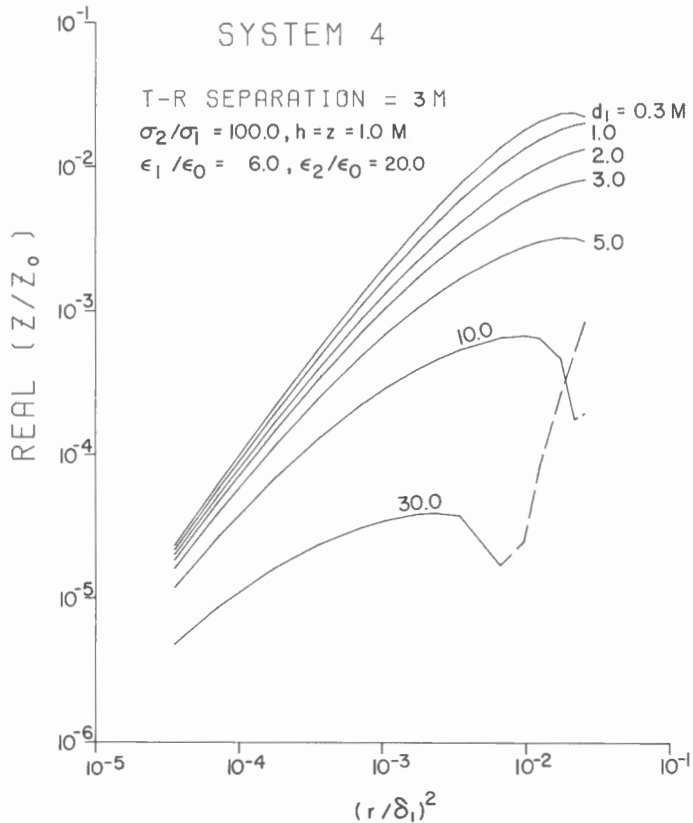


Figure 8. Variation of real (Z/Z_0) against $(r/\delta_1)^2$ for System 4 over several two layer models for a coil separation of 3 m.

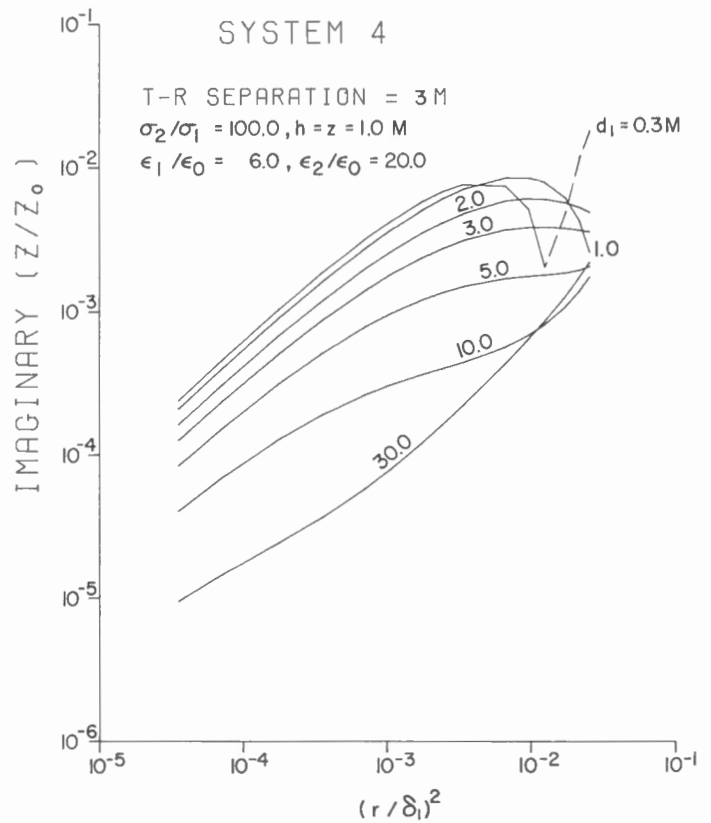


Figure 9. Variation of imaginary (Z/Z_0) against $(r/\delta_1)^2$ for System 4 over several two layer models for a coil separation of 3 m.

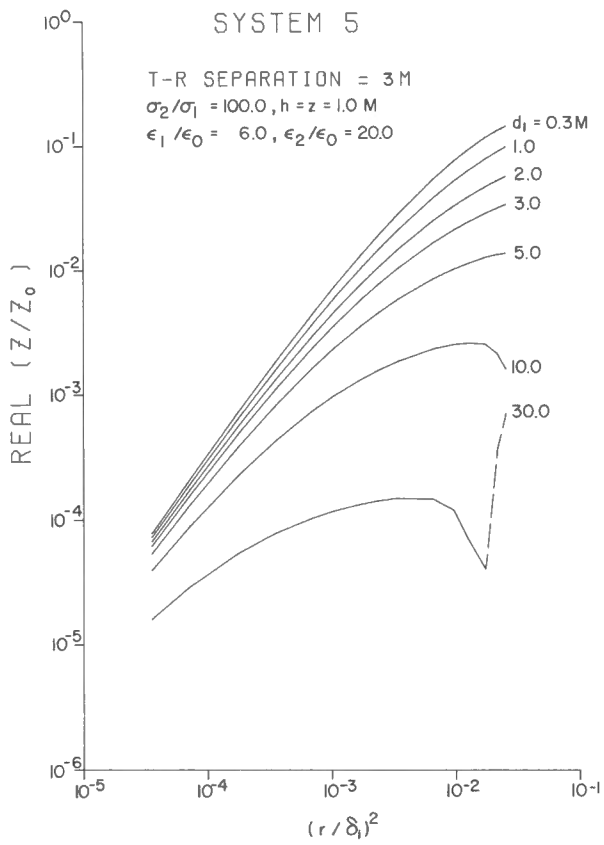


Figure 10. Plot of real (Z/Z_0) versus $(r/\delta_1)^2$ for several two layer models for a coil separation of 3 m in System 5.

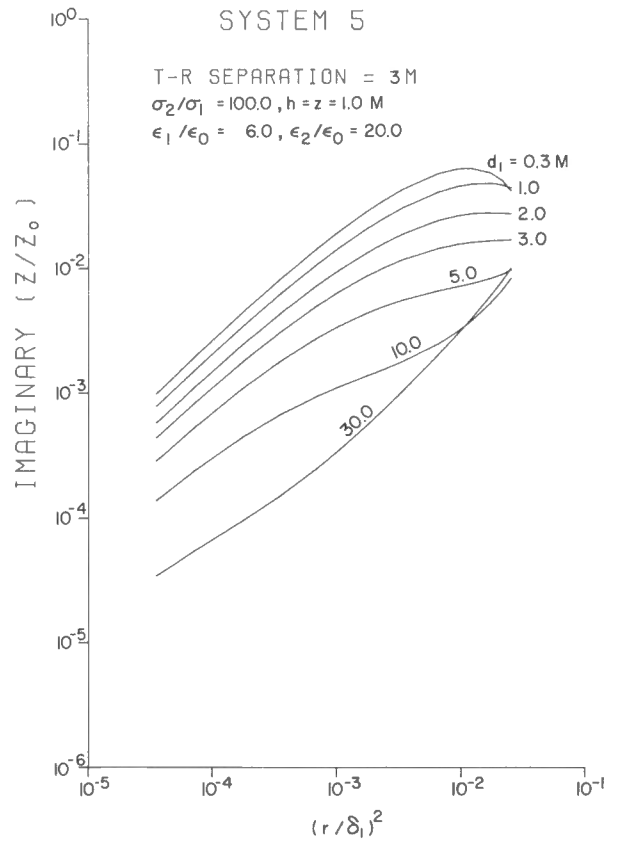


Figure 11. Plot of imaginary (Z/Z_0) versus $(r/\delta_1)^2$ for several two layer models for a coil separation of 3 m in System 5.

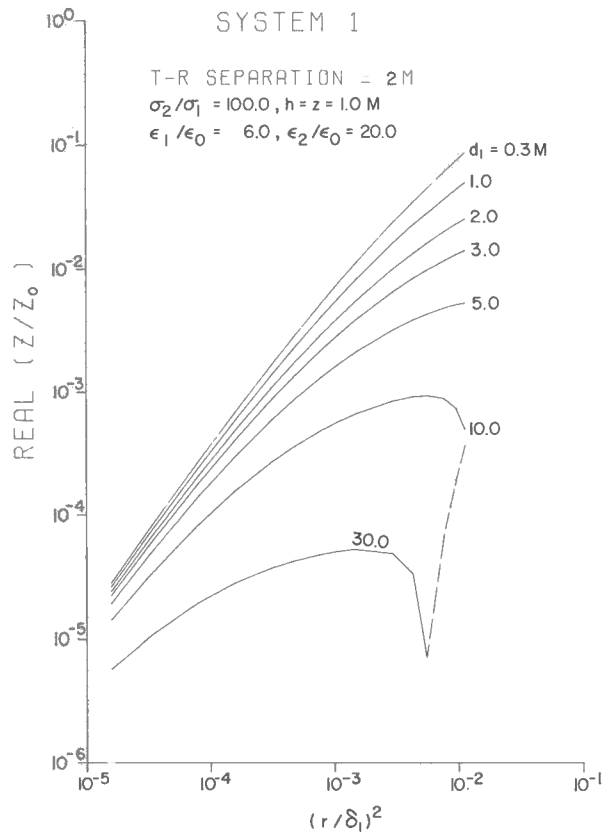


Figure 12. Effect of decreasing coil separation on real (Z/Z_0) for System 1.

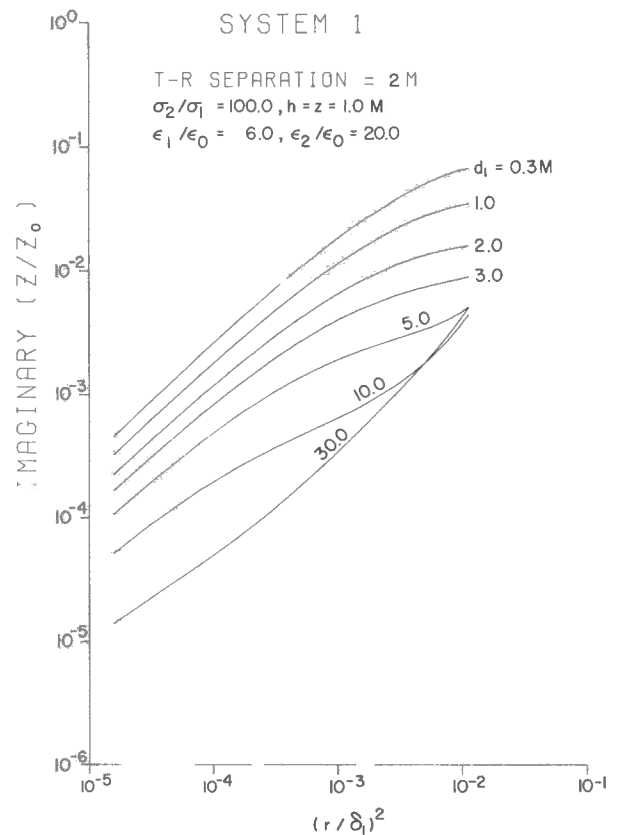


Figure 13. Effect of decreasing coil separation on imaginary (Z/Z_0) for System 1.

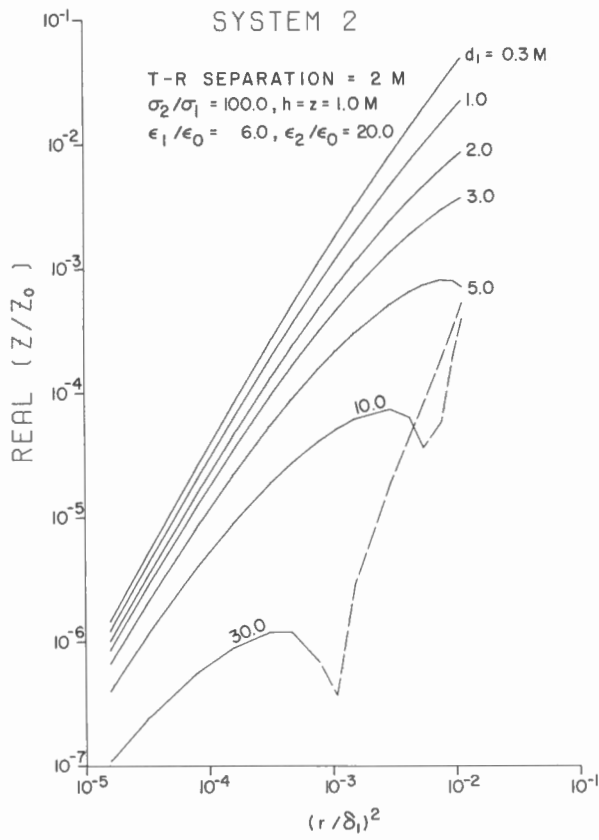


Figure 14. Effect of decreasing coil separation on real (Z/Z_0) for System 2.

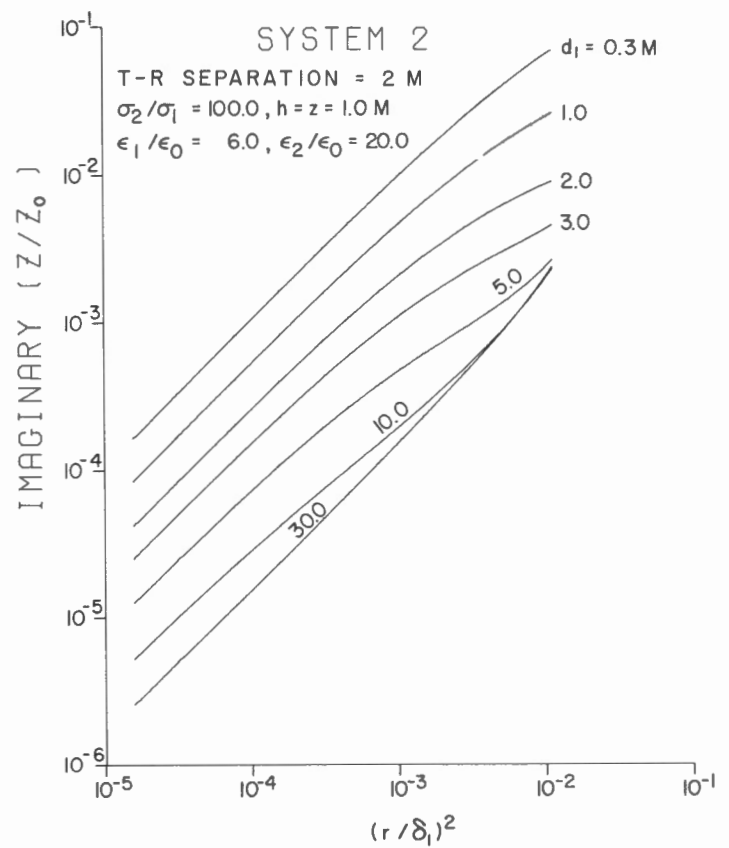


Figure 15. Effect of decreasing coil separation on imaginary (Z/Z_0) for System 2.

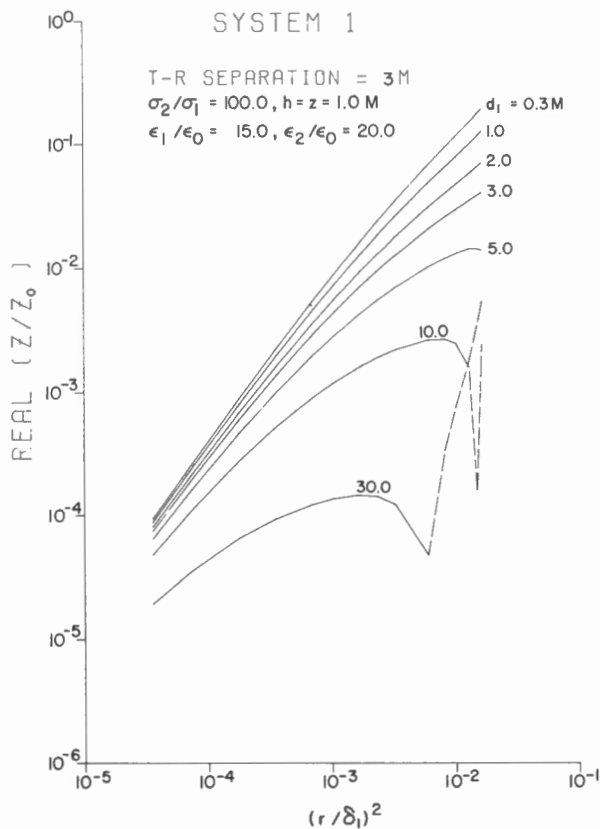


Figure 16. Effect of changing the dielectric constant of the top layer on real part of (Z/Z_0) for System 1.

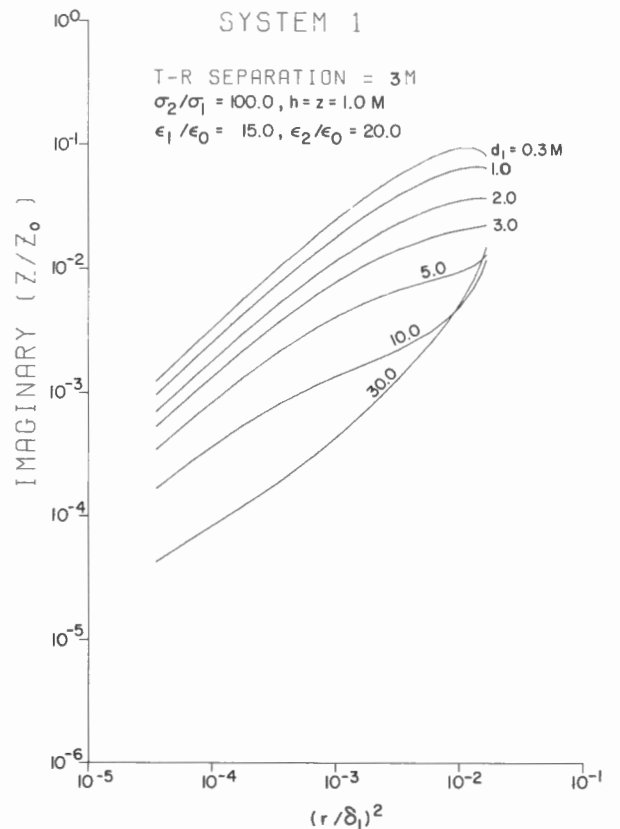


Figure 17. Effect of changing the dielectric constant of the top layer on the imaginary part of (Z/Z_0) for System 1.

Figures 4 and 5 show a similar plot for System 2 for the same set of variables. The curves are quite similar in appearance to Figures 2 and 3 but the range of variation of (Z/Z_0) values over the frequency range in this case is higher. The highest values of (Z/Z_0) in the two systems are almost the same, but the lowest values are less in System 2. It means that at lower frequencies the signal may be below the noise level (5-10 ppm) and frequencies below 10 Khz may not be usable. But the resolution seems to be better in this system. Figures 6 and 7 show the variations in System 3. The range of variation of values in this system fall between those for Systems 1 and 2. In all three systems, the negative values (dashed sections) occur in the real part for high frequency and d_1 values. This agrees with the results published previously for homogeneous media (Sinha, 1976a).

Figures 8 and 9 show the results for System 4. The range of values in this system are about an order less than in the three previous systems. Another interesting feature is the presence of negative values in imaginary (Z/Z_0) for very thin top layers at higher frequencies. Figures 10 and 11 illustrate the variations of the real and imaginary parts of (Z/Z_0) for System 5. The graphs are similar to those for System 1 although the range of variations is somewhat less. It appears, therefore, that mutual coupling values are highest in System 1 but the range of variation and resolution is higher in System 2. System 5 is a close second behind System 1 in terms of the amplitudes of the mutual coupling ratios.

To examine the effects of coil separation on the results, we have plotted the results for a separation of 2 m for System 1 in Figures 12 and 13 keeping all other variables identical. As expected, both real and imaginary parts of (Z/Z_0) are consistently smaller than the corresponding values for the coil separation of 3 m, although there should be no problem in measuring them since the values are almost always greater than 10 ppm. Figures 14 and 15 illustrate the variations for a coil separation of 2 m for System 2. As in the previous diagram with coil separation of 3 m, the anomaly values are less in this system, specially for larger d_1 values. In fact, at lower frequencies, the real anomaly values are often less than 1 ppm. This means that it will be difficult to use this system at lower than 3 m coil separation in permafrost terrain as the signal should be at least 10 ppm for meaningful interpretation.

The last two plots (Figs. 16 and 17) illustrate the influence of changing the dielectric constant of the top layer from 6 to 15 on the mutual coupling values. The effect seems to be minimal at lower frequencies since the displacement current effects are negligible in that region. Even at higher frequencies, as long as the top layer is thin, the effects are small since the bottom layer effects are generally predominant. However, when d_1 is 10 m or more, the displacement current effects are quite significant at the higher frequency ends. For the real part, the effect is to move the values more towards the negative end as the ϵ_1/ϵ_0 values are increased. This effect was seen previously in case of homogeneous dielectrics too. Effects of changing the conductivity contrast σ_2/σ_1 on the (Z/Z_0) values have not been shown here since an increase in σ_2/σ_1 appears to increase the magnitude of the response only without changing the curve shapes, so that the separation between different lines for different d_1 values increase and vice versa.

In all the simulations, the variation of electrical properties with frequency has not been considered, although it is known that they do vary in the frequency range of our interest. That effect would be considered in a forthcoming paper (Sinha, 1977b). However, the theoretical results and the accompanying computer program would be useful where the frequency variations are not severe.

CONCLUDING REMARKS

From the numerical results presented in this paper, it would appear that the horizontal coplanar system (System 1) would possibly be best for mapping layered permafrost terrain. A coil separation of 3 m would seem to be optimum from the viewpoint of portability and reasonably high anomalies that should be recorded if the coils are held 1 m above the surface. The inclined parallel system (System 5) comes a close second, while System 4 appears to be the worst. For resolution, however, the perpendicular system (System 2) is probably the best but the signal level would be rather low in this system at lower frequencies.

Permafrost mapping has been attempted with several electromagnetic techniques in the past with varying success. Since there are ample lateral inhomogeneities in permafrost terrain, any large scale system (where the distance between the source and receiver is large) would tend to integrate the total effect and details would be lost. The double-dipole and radar systems appear to be two systems capable of mapping the fine details in permafrost terrain. However, the radar systems are expensive and not very portable. A double dipole e.m. system with 2-3 m coil separation would be excellent from the point of view of portability, cost and quality of coverage.

In the interpretation of e.m. sounding data over layered lossy dielectric terrain like permafrost, we need to know the theoretical response of various layered lossy dielectric models. However, since the number of possible parameters for such a medium will be large, it would be futile trying to publish master-charts for them. The only practical way is to have a generalized computer program so that the interpreter can generate the theoretical curve for any set of input data for matching with the field data. Such a generalized computer program has been included in the Appendix. The program may be used interactively on a graphic screen (Sinha, 1976b) or otherwise for interpreting any dipole e.m. sounding data.

REFERENCES

- Abramowitz, M. and Stegun, I.A.
1965: Handbook of mathematical functions; Dover Publications Inc., New York.
- Ananyan, A.A.
1958: Dependence of electrical conductivity of frozen rocks on moisture content; Bull. Acad. Sci. USSR, Geophys. Ser., no. 12, p. 878-881.
- Annan, A.P. and Davis, J.L.
1976: Impulse radar sounding in permafrost; Radio Science, v. 11, no. 4, p. 383-394.
- Collett, L.S. and Becker, A.
1968: Radiohm method for earth resistivity surveying; Canadian Patent No. 795, 919, Oct. 1.
- Dey, A. and Ward, S.H.
1970: Inductive sounding of a layered earth with a horizontal magnetic dipole; Geophysics, v. 35, no. 4, p. 660-703.
- Ferrians, O.J. and Hobson, G.D.
1973: Mapping and predicting permafrost in North America; A review, 1963-1973; Proc., The North American Contribution to the Second Int. Conf. on Permafrost, NRC-NAS, p. 479-498.
- Frischknecht, F.C.
1967: Fields about an oscillating magnetic dipole over a two-layer earth and application to ground and airborne electromagnetic surveys; Colo. Sch. Mines, Q., v. 62, no. 1, 326 p.
- Hoekstra, P., Sellmann, P.V. and Delaney, A.
1975: Ground and airborne resistivity surveys of permafrost near Fairbanks, Alaska; Geophysics, v. 40, no. 4, p. 641-656.
- Koziar, A. and Strangway, D.W.
1975: Magnetotelluric sounding of permafrost; Science, v. 190, p. 566-568.
- Mackay, D.K.
1969: Electrical resistivity measurements in frozen ground, Mackenzie Delta area, N.W.T.; Assoc. Int. Hydro. Sci., Acts du Colloque de Bucarest, Paris.
- Sinha, A.K.
1973: Comparison of airborne e.m. coil systems placed over a multilayer conducting earth; Geophysics, v. 38, no. 5, p. 894-919.
- 1974: Electromagnetic sounding in permafrost regions; in Report of Activities, Part B, Geol. Surv. Can., Paper 74-1B, p. 109-110.
- 1976a: Determination of ground constants of permafrost terrains by an electromagnetic method; Can. J. Earth Sci., v. 13, no. 3, p. 429-441.
- 1976b: An interactive graphic system for interpretation of dipole e.m. sounding data; in Report of Activities, Part C, Geol. Surv. Can., Paper 76-1C, p. 51-53.
- 1977a: Influence of altitude and displacement currents on plane wave e.m. fields; Geophysics, v. 42, no. 1, p. 77-91.
- 1977b: A theoretical study on electromagnetic probing of permafrost terrains. Under publication in Can. J. Earth Sci. (in press).
- Sinha, A.K. and Collett, L.S.
1973: Electromagnetic fields of oscillating magnetic dipoles placed over a multilayer conducting earth; Geol. Surv. Can., Paper 73-25, 48 p.
- Wait, J.R.
1966: Fields of a horizontal dipole over a stratified anisotropic half-space; I.E.E. Trans. on Ant. Prop., v. AP-14, no. 11, p. 790-792.

APPENDIX

COMPUTER PROGRAM FOR COMPUTING THE ELECTROMAGNETIC RESPONSE
OF AN N-LAYER LOSSY DIELECTRIC EARTH IN FIVE STANDARD COIL SYSTEMS
USED BY THE GEOPHYSICAL INDUSTRY

```

1  PROGRAM COMPTI (INPUT, OUTPUT, IAPF5=INPUT, IAPF6=OUTPUT)
C *****
C PROGRAM TO COMPUTE THE REAL AND IMAGINARY PARTS AND ALSO THE
C AMPLITUDE AND PHASE OF THE SECONDARY FIELDS OF HORIZONTAL AND
C VERTICAL MAGNETIC DIPOLES OVER AN N-LAYER LOSSY DIELECTRIC EARTH.
C IAPF5 = INPUT MEANS THAT THE VALUES ARE TO BE FOUND ON THE CARD HEADER.
C IAPF6 = OUTPUT MEANS THAT THE VALUES SPECIFIED ARE TO BE PLACED
C ON THE LINE PRINTER.
C *****
10 C *****
C THIS PROGRAM HAS BEEN DEVELOPED BY AJIT K. SINHA OF ELECTRICAL
C METHODS SECTION, GEOLOGICAL SURVEY OF CANADA, OTTAWA, CANADA.
C *****
15 C *****
C DEFINITIONS OF THE DIFFERENT PARAMETERS USED
C NUM = NUMBER OF LAYERS OF THE EARTH SECTION
C RH = SEPARATION BETWEEN THE TRANSMITTER AND THE RECEIVER
C *****
20 C *****
C LOOPS IN METERS
C S1 = THE CONDUCTIVITY OF THE TOPMOST LAYER IN S/M
C K(M) = VALUES OF SIGMA(M)/S, WHERE SIGMA(M) IS THE CONDUCTIVITY
C OF THE MTH LAYER. THE VALUES OF K(M) START FROM THE BOTTOMMOST
C LAYER (LARGEST M) AND GO UPWARDS TO THE VALUE OF K(1) = 1.
C H = COIL ELEVATIONS IN METERS
C *****
25 C *****
C ELEVATION OF THE COILS OVER THE GROUND IS ASSUMED TO BE 1 METER
C IN THIS PROGRAM, HOWEVER ANY VALUE OF H MAY BE ASSIGNED
C FRE = FREQUENCY IN HERTZ
C D(M) = THICKNESS OF THE LAYERS STARTING WITH THE BOTTOMMOST VALUE
C FIRST, THAT IS D(M) = 0., AND THEN GRADUALLY MOVING UPWARDS.
C E(M) = DIELECTRIC CONSTANTS OF THE MTH LAYER STARTING WITH THE
C BOTTOMMOST LAYER AND GRADUALLY MOVING UPWARDS
C OPT = AN INTEGER PARAMETER. OPT IS EQUAL TO 0 WHEN TRANSVERSE
C ELECTRIC (TE) MODE IS BEING CONSIDERED AND IT IS EQUAL TO 1
C WHEN TRANSVERSE MAGNETIC (TM) MODE IS BEING CONSIDERED.
C DEL = SKIN DEPTH IN METRES IN THE TOP LAYER
C *****
35 C *****
C *****
C *****
40 C *****
C XX VALUES INDICATE THE FREQUENCY VALUES IN HERTZ
C DIMENSION THE REAL VALUE ARRAYS K, D AND F VALUES
C *****
C *****
C *****
45 DIMENSION XX(20), X(20), Z(20), RE(20), QD(20), RF(20), QF(20), RG(20)
DIMENSION JG(20), PT(20), QT(20), RM(20), NM(20), R7(20), QZ(20)
DIMENSION RA1(20), RA2(20), RA3(20), RA4(20), RA5(20)
DIMENSION AIM1(20), AIM2(20), AIM3(20), AIM4(20), AIM5(20)
DIMENSION PIM1(20), PA1(20), PA2(20), PA3(20), PA4(20), PA5(20)
COMPLEX KA, PB, RC, RP, RR
C *****
50 COMPLEX R1(20), R2(20), R3(20), R4(20), R5(20), R6(20)
REAL X(8), D(8), E(8)
INTEGER IFF, OPT
PIE = 3.14159265359
C *****
55 C *****
C REPRESENTATION OF XX ARRAYS AS DATA INPUT (FREQUENCY)
C *****
C *****
DATA XX/1000., 2000., 3000., 40000., 50000., 10000., 20000., 30000., 50000., 70000.,
110000., 200000., 300000., 400000., 500000., 800000., 1000000./
DATA M/15/

```

```

*****
C WRITE THE ORIGINAL TITLE ON THE LINE PRINTER.
C*****
WRITE (6,189)
65 189 FORMAT (1H,*, E.M. DIPOLE SOUNDING RESULTS OVER PERMAFROST **/)
C*****
C READ THE DATA VALUES REQUIRED FOR SUBSEQUENT CALCULATIONS
C*****
42 READ (5,100) (NUM,RH,SI,K(J),J=1,NUM)
100 FORMAT (12,7F10.0)
101 FORMAT (7F10.0)
75 102 FORMAT (7F10.0)
IF (RH.GT.200.) GO TO 43
C*****
C THE LAST DATA CARD MUST HAVE RH GREATER THAN 200 TO END THE JOB.
C*****
80 *****
C*****
C WRITE THE INITIAL DATA VALUES THAT HAVE JUST BEEN READ
C*****
WRITE (6,103)
85 103 FORMAT (1H,*, NO. OF LAYERS,COIL SEP., SIGMAI ,AND SIGM/SIGI
1 VALUES FROM BOTTOM UPWARDS **/)
WRITE (6,104) (NUM,RH,SI,K(J),J=1,NUM)
104 FORMAT (1H,14,7F12.3/)
WRITE (6,105)
90 105 FORMAT (1H,*, THICKNESSES OF LAYERS IN METERS FROM BOTTOM UP
WARDS **/)
WRITE (6,106) (D(J),J=1,NUM)
106 FORMAT (3X,7F15.2/)
WRITE (6,107)
95 107 FORMAT (1H,*, DIELECTRIC CONSTANTS OF THE LAYERS FROM BUTTO
M UPWARDS **/)
WRITE (6,108) (E(J),J=1,NUM)
108 FORMAT (3X,7F15.2/)
E1= E(NUM)
DC= 8.854*(1.E-12)
H= 1.
DO 400 I=1,M
FRE= XX(I)
OMEG= 2.*PIE*FRE
OME= SI/(OMEG*DC*F1)
RS= SORT(1.+OME*OMF)
RQ= 2./(F1*(1.-RS))
QQ= 2.*OME/(RS-1.)
OMU= 2.*PIE*8.854*(1.E-10)
DEL= J./(OMEG*SORT(OMU*F1*(RS-1.)))
A= 2.*H/DEL
B= RH/DEL
PI2= PIE**2
CS= 4.*PI2*FRE*DEL/(1.E-7)
115 PD= SORT(-RR)
RRX= CMLX(0.0,MD)
RP= B*RRR
RQ= A*RR*RR
RA= 1.+RP*RR

```

```

120 RB= 1.*RP
      RC= CEXP(RP)
      C*****
      C OPT= 0 MEANS THAT THE TEE COMPONENT IS INVOLVED IN THE NUMERICAL
      C INTEGRATION OF THE INFINITE INTEGRALS.
      C*****
125 X(I)= R
      C*****EVALUATION OF THE INTEGRAL I0 *****
      OPT= 0
      TEE= 0
130 CALL SUBM (TEE,OPT,R,D,R,K,E,RR,QQ,CS,NUM,DEL,A,TREAL,TIMAG)
      RE(I)= -TREAL
      QD(I)= -TIMAG
      RI(I)= CMLPX(RE(I),QD(I))
      C*****EVALUATION OF THE INTEGRAL T1 *****
135 OPT= 0
      TEE= 1
      CALL SUBM (TFE,OPTI,R,D,R,K,E,RR,QQ,CS,NUM,DEL,A,TREAL,IMAI)
      RF(I)= -TREAL
      QF(I)= -TMAI
      R2(I)= CMLPX(RF(I),QF(I))
      C*****EVALUATION OF THE INTEGRAL I2 *****
140 OPT= 1
      TEE= 2
      CALL SUBM (TEE,OPT,R,D,R,K,E,RR,QQ,CS,NUM,DEL,A,TREA2,TIMA2)
      RG(I)= -TREA2
      QG(I)= -TIMA2
      R3(I)= CMLPX(RG(I),QG(I))
      C*****EVALUATION OF THE INTEGRAL I3 *****
145 OPT= 0
      TEE= 3
      CALL SUBM (TFE,OPTI,R,D,R,K,E,RR,QQ,CS,NUM,DEL,A,TREA3,IMA3)
      RT(I)= -TREA3
      QT(I)= -TMA3
      R4(I)= CMLPX(RT(I),QT(I))
      C*****EVALUATION OF THE INTEGRAL I4 *****
155 OPT= 1
      TEE= 4
      CALL SUBM (TEE,OPT,R,D,R,K,E,RR,QQ,CS,NUM,DEL,A,TREA4,TIMA4)
      RM(I)= -TREA4
      QM(I)= -TIMA4
      R5(I)= CMLPX(RM(I),QM(I))
      C*****EVALUATION OF THE INTEGRAL I5 *****
160 OPT= 0
      TEE= 5
      CALL SUBM (TFE,OPTI,R,D,R,K,E,RR,QQ,CS,NUM,DEL,A,TREA5,IMA5)
      RZ(I)= -TREA5
      QZ(I)= -TMA5
      R6(I)= CMLPX(RZ(I),QZ(I))
      C*****
170 C*****
      C COMPLEX MUTUAL COUPLING RATIOS IN THE FIVE SYSTEMS
      C*****
      Q1(I)= R**3**R1(I)**RC/RA
      Q2(I)= R**3**R4(I)**RC/RA
      Q3(I)= (R**8*(R5(I)+R5(I)-R**R3(I)))*RC/RA
      Q4(I)= -(R**8*(R6(I)+P5(I)-R**R2(I)))*RC/(2.*RB)
      Q5(I)= -R**8*(R5(I)+R5(I)-R*(R2(I)+2.*R1(I)))*RC/(3.*RA)
      C*****
175

```

```

C REAL PARTS OF THE (Z/70) VALUE IN FIVE SYSTEMS
C RA1,RA2 ETC. REPRESENT REAL PARTS OF (Z/70) IN P.P.M.
C *****
180 RA1(I)= REAL(Q1(I))*(1.E 6)
RA2(I)= REAL(Q2(I))*(1.E 6)
RA3(I)= REAL(Q3(I))*(1.E 6)
185 RA4(I)= REAL(Q4(I))*(1.E 6)
RA5(I)= REAL(Q5(I))*(1.E 6)
C *****
C IMAGINARY PARTS OF THE (Z/70) RATIOS IN FIVE SYSTEMS
C IM1,AIM2 ETC. REPRESENT IMGINARY PARTS OF (Z/70) IN P.P.M.
C *****
190 AIM1(I)= AIMAG(Q1(I))*(1.F 6)
AIM2(I)= AIMAG(Q2(I))*(1.F 6)
AIM3(I)= AIMAG(Q3(I))*(1.F 6)
AIM4(I)= AIMAG(Q4(I))*(1.F 6)
195 AIM5(I)= AIMAG(Q5(I))*(1.F 6)
C *****
C COMPUTATION OF THE AMPLITUDE AND PHASE VALUES IN DEGREES
C PIM1,PIM2 ETC. ARE AMPLITUDE VALUES IN SYSTEMS 1,2 ETC.
C PA1,PA2 ETC. ARE PHASE VALUES(DEGREES) IN SYSTEMS 1,2 ETC.
C *****
200 PIM1(I)= SQRT(RA1(I)**2+AIM1(I)**2)
PIM2(I)= SQRT(RA2(I)**2+AIM2(I)**2)
PIM3(I)= SQRT(RA3(I)**2+AIM3(I)**2)
PIM4(I)= SQRT(RA4(I)**2+AIM4(I)**2)
PIM5(I)= SQRT(RA5(I)**2+AIM5(I)**2)
PA1(I)= ATAN2(AIM1(I),RA1(I))*180./PIE
PA2(I)= ATAN2(AIM2(I),RA2(I))*180./PIE
PA3(I)= ATAN2(AIM3(I),RA3(I))*180./PIE
PA4(I)= ATAN2(AIM4(I),RA4(I))*180./PIE
PA5(I)= ATAN2(AIM5(I),RA5(I))*180./PIE
Z(I)= R**H
400 CONTINUE
C *****
C PRINT ALL THE FINAL RESULTS AT ALL FREQUENCIES
C *****
215
C
220 199 WRITE (5,199)
FORMAT (1H , * B RA1 RA2 RA3 RA4 RA5
X AIM2 AIM3 AIM4 AIM5 */)
1) ,RA4(I),AIM4(I),RA5(I),AIM5(I),I= 1,M)
200 FORMAT (2X,F8.6,2X,10E12.6)
WRITE (6,299)
225 299 FORMAT (1H , * B-SOP PH1 PH2 PH3 PH4 PH5
X AMP2 AMP3 AMP4 AMP5 */)
WRITE (6,288) ((Z(I),PA1(I),PIM1(I),PA2(I),PIM2(I),PA3(I),PIM3(I),
1),PA4(I),PIM4(I),PA5(I),PIM5(I)),I= 1,M)
288 FORMAT (2X,F8.6,2X,10E12.6)
C *****
C INSTRUCTION TO GO TO STATEMENT 42 TO READ ANOTHER INPUT DATA CARD
C *****
235 43 STOP
END

```

```

1 SUBROUTINE SUBM(TEF,OPT,R,D,F,K,E,RR,QQ,CS,NUM,DEL,C,TREAL,TIMAG)
C*****
C THIS SUBROUTINE CALCULATES THE INFINITE INTEGRALS TO.II .....TS.
C THIS IS CALLED FROM THE MAIN PROGRAM COMPUT SIX TIMES FOR EACH
C DATA SET READ IN THE MAIN PROGRAM.
C*****
DIMENSION P(10),Q(10),R(10),S(10),THE(10),ETA(10)
DIMENSION AV(50),X(50)
REAL AW(96),W(96),X0(45),X1(45),AREAR(100),AREAI(100),Z(100)
INTEGER TEE,L,I,M,N,N21,KI,JI,OPT,JJ,KJ
REAL A,R,EPS,MU, J0X,J1X,JK
REAL O(10),K(10),F(10)
LOGICAL BOOL
COMPLEX T(20),TA(20),PA(20),YA(20),PAA(20),PAB(20)
COMPLEX PR(20),ZA(20),SAA(20),SAB(20)
COMPLEX EX,WEX,GGY
COMPLEX YE,PE,ZE,SF,SJ,JWEX
COMPLEX GK,RF1,RG1
C*****
C OPT MAY BE 0 OR 1 FOR THE TF OR THE TM MODE CASE
C*****
C
C AW VALUES REPRESENT THE AHSCISSA VALUES X(I), WHERE X(I) IS THE ITH
C ZERO OF THE LEGENDRE POLYNOMIAL P_N.
C W VALUES REPRESENT THE WEIGHT FACTORS W(I).
C X0 AND X1 ARE THE POSITIONS OF THE ZEROS OF THE BESSEL FUNCTIONS
C J0 AND J1. FORTYFIVE VALUES OF THEM HAVE BEEN CONSIDERED.
C*****
C
C
C
30 DATA AW/ .99968950388, .99836437586, .99598184298, .99254390032,
A .98805412633, .98251726356, .97593917458, .96832682846,
R .95968829144, .95003271778, .93937033975, .92771245672,
C .91507142312, .90146063531, .88689451740, .87138850590,
D .85495903343, .83762351122, .81940031073, .80030874414,
E .78036904386, .75960234117, .73803064374, .71567681235,
F .69256453664, .66871931004, .64416340378, .61992584012,
G .59303236477, .56651041856, .53936810832, .51169417715,
H .48345797392, .45470942216, .42547898840, .39579764982,
P .36569686147, .33520852289, .30436494435, .27319891259,
Q .24174315616, .21003131046, .17809688236, .14597371465,
R .11369585011, .08129749546, .04881298513, .01627674485 /
DATA AV/ -.99968950388, -.99836437586, -.99598184298, -.99254390032,
T -.98805412633, -.98251726356, -.97593917458, -.96832682846,
U -.95968829144, -.95003271778, -.93937033975, -.92771245672,
1 -.91507142312, -.90146063531, -.88689451740, -.87138850590,
2 -.85495903343, -.83762351122, -.81940031073, -.80030874414,
3 -.78036904386, -.75960234117, -.73803064374, -.71567681235,
4 -.69256453664, -.66871931004, -.64416340378, -.61992584012,
5 -.59303236477, -.56651041856, -.53936810832, -.51169417715,
6 -.48345797392, -.45470942216, -.42547898840, -.39579764982,
7 -.36569686147, -.33520852289, -.30436494435, -.27319891259,
8 -.24174315616, -.21003131046, -.17809688236, -.14597371465,
9 -.11369585011, -.08129749546, -.04881298513, -.01627674485 /
DATA W/.00079679205, .00185396078, .00291073181, .00395455434,
A .00501420274, .00605954550, .00709647079, .00812587692,
B .00914867123, .01016077053, .01116210210, .01215160467,

```

```

C .01312322956,.01409094177,.01503872102,.0157056290,
D .01688547986,.01774250231,.01866067962,.01951908114,
E .02035679715,.02117273949,.02196664444,.02273706965,
F .02348339908,.0242044179,.02490063322,.02557003600,
G .02621234073,.02688269672,.02741296272,.02797000761,
H .02849741106,.02899401415,.02946108995,.02989634413,
P .03029991542,.03067137612,.03101033258,.03131642559,
Q .03158933077,.03192875889,.03203445623,.03220620479,
R .03234382256,.03244716371,.03251611871,.03255061449/
DATA X/.00079679206,.00185396078,.00291073181,.00396455434,
T .00501420274,.00605854550,.00709647079,.00812687692,
U .00914867123,.01016077053,.01115210210,.01215160467,
1 .01312822456,.01409094177,.01503872102,.01597056290,
2 .01688547986,.01774250231,.01866067962,.01951908114,
3 .02035679715,.02117273949,.02196664444,.02273706965,
4 .02348339908,.0242044179,.02490063322,.02557003600,
5 .02621234073,.02688269672,.02741296272,.02797000761,
6 .02849741106,.02899401415,.02946108995,.02989634413,
7 .03029991542,.03067137612,.03101033258,.03131642559,
8 .03158933077,.03192875889,.03203445623,.03220620479,
9 .03234382256,.03244716371,.03251611871,.03255061449/
DO 100 I= 1,44
J= I+ 48
AW(J)= AV(I)
W(J)= X(I)
100 CONTINUE
DATA X0/2,4,048255577,5,5200781103,8,5537279129,11,7915344439,
1 14,939017708,18,071063968,21,211636630,24,352471531,
2 27,493479132,30,634606468,33,775820214,36,917098354,
3 40,058425765,43,199791713,46,341188372,49,482609897,
4 52,624051841,55,765510755,58,906983926,62,048469190,
5 60,1899648,68,3314593,71,4729816,74,6145006,77,7560256,
6 80,8975559,84,0390908,87,1806298,90,3221726,93,4637188,
7 96,6052680,99,7468199,102,8883743,106,0299309,109,1714896,
8 112,3130503,115,4545127,118,5961766,121,7377421,124,8793089,
9 128,0207769,131,1624460,134,3040161,137,4455871,140,5871589/
DATA X1/3,83170597,7,01558667,10,17346814,13,32369194,16,47063605,
1 19,61585851,22,76008438,25,90367209,29,04682853,32,18967991,
2 35,33230755,38,47476623,41,61709421,44,75931900,47,90146089,
3 51,04353518,54,18555364,57,32752544,60,46945785,63,61135670,
4 66,7532267,69,8950718,73,0368952,76,1786996,79,3204872,
5 82,4622599,85,6040194,88,7457671,91,8975043,95,0292318,
6 98,1709507,101,3126618,104,4543658,107,5960633,110,7377548,
7 113,8794408,117,0211214,120,1627983,123,3044705,126,4461387,
8 129,5878031,132,7294639,135,8711213,139,0127755,142,1544267/
DATA M,N/96,447
C
C *****
C CHECK INPUTS HERE
C M IS THE NUMBER OF SURDIVISIONS WITHIN THE AREA BOUNDED BY TWO
C CONSECUTIVE ZEROS OF THE BESSEL FUNCTION AND N IS THE NUMBER
C OF SUCH SEGMENTS.
C *****
C IF (TEE,L,I,0,OR,IFE,GT,5,OR,R,EQ,0,) RETURN
L=1
IF (TEE,EQ,0,OR,IFE,EQ,1,OR,IFE,EQ,2) GO TO 60

```

```

115      DO 50 I=1,N
          Z(I) = X1(I)/R
          GO TO 90
        C
          60      DO 70 I=1,N
          70      Z(I) = X0(I)/R
        C
          90      CONTINUE
          SUMR=0.
          SUMI=0.
          IF (L.EQ.1) GO TO 95
          GL=GU
          GU=Z(L)
          GO TO 98
          95      GL=0.
          GU=Z(1)
          98      MU=.5*(GU-GL)
        C
          DO 900 I=1,M
          C***** CALL FUNCTION GG *****
          135      G= GG(AW(I),GU,GL)
          G2= G*G
          G3= G2*G
          GZZ= G2 +RR
          IF (GZZ .LT. 0. ) GO TO 129
          140      GZ= SQRT (GZZ)
          GK= CMPLX(GZ,0.0)
          GY= C*GZ
          EX= EXP(-GY)
          GO TO 130
          145      129      GZ1= -GZZ
          GY2= SQRT(GZ1)
          GK= CMPLX(0.,GYZ)
          GYY= C*GK
          EX= CEXP(-GY)
          150      130      IF (OPT .NE. 0) GO TO 701
          C*****
          C THIS CASE CORRESPONDS TO THE TE MODE REFLECTION COEFFICIENT
          C*****
          DO 200 JI= 1,N(JM)
          155      KK= K(JI)
          EE= E(JI)
          DD=D(JI)/ZDEL
          U= G2+ RR*EE
          V= QQ*KK
          UV= SQRT((U+V*V)
          IF ( KK .FO. 0. ) GO TO 499
          ALP= SQRT(0.5*(U+UV) )
          BEI= V/(2.*ALP)
          GO TO 599
          165      499      IF (U .LT. 0. ) GO TO 799
          ALP= SQRT(U)
          BEI= 0.
          GO TO 599
          799      ALP= 0.
          170      599      P(JI)= BEI/CS

```

```

Q(JI)=-ALP/CS
PA(JI)=CMPLX(P(JI),U(JI))
IF (JI.EQ.1) GO TO 200
175 R(JI)=2.*DD*ALP
IF ( R(JI) .GT. 40.) R(JI) =40.
S(JI)=2.*DD*BET
IF ( S(JI) .GT. 40.) S(JI) =40.
T(JI)=CMPLX (P(JI),S(JI))
180 TA(JI)=(1.-CEXP(-T(JI)))/(1.+CEXP(-T(JI)))
200 CONTINUE
DO 250 KI= 1,NUM
IF (KI.NF.1) GO TO 16
YA(KI)= PA(KI)
185 GO TO 250
PAA(KI)= PA(KI)*TA(KI)
PAB(KI)= YA(KI-1)*TA(KI)
YA(KI)= PA(KI)*(YA(KI-1)+PAA(KI))/(PA(KI)+PAB(KI))
250 CONTINUE
YE= YA(NUM)
190 IF (GZZ .LT. 0.) GO TO 534
GZCS= GZ/CS
PE= CMPLX(0.0,-GZCS)
195 RFI= (PE-YE)/(PE+YE)
534 GYCS= GYZ/CS
RFI= (GYCS-YE)/(GYCS+YE)
535 GO TO 600
C*****
C THIS CASE CORRESPONDS TO THE TM MODE REFLECTION COEFFICIENT
C*****
701 DO 300 JJ= 1,NUM
PJ= K(JJ)
EJ= E(JJ)
205 DJ= D(JJ)/DEL
U= G2*RR*EJ
V= QQ*PJ
UV= SURT(U*U+V*V)
210 IF (PJ .EQ. 0.) GO TO 498
ALP= SURT(0.5*(U+UV))
RET= V/(2.*ALP)
GO TO 598
498 IF (U .LT. 0.) GO TO 798
ALP= SURT(U)
BET= 0.
215 GO TO 598
798 ALP= 0.
BET= SURT(-U)
220 THE1= ALP*RR*EJ +BET*V
ETAI= BET*RR*EJ-ALP*V
DENO= (RR*EJ)**2+V*V
THE(JJ)= -CS*ETAI/DENO
ETA(JJ)= CS*THE1/DENO
PB(JJ)= CMPLX(TH(JJ),ETA(JJ))
225 IF (JJ .FO. 1) GO TO 300
R(JJ)= 2.*DJ*ALP
IF ( R(JJ) .GT. 40.) R(JJ) =40.
S(JJ)= 2.*DJ*BET

```

```

230 IF ( S(JJ) .GT. 40.) S(JJ) =40.
      T(JJ)= CMLX(R(JJ)*S(JJ))
      TA(JJ)= (1.-CEXP(-T(JJ)))/(1.*CEXP(-T(JJ)))
      CONTINUE
      DO 350 KJ= 1,NUM
      IF (KJ .NE.1) GO TO 88
      ZA(KJ)= PB(KJ)
      GO TO 350
      88 SAA(KJ)= PB(KJ)*TA(KJ)
      SAB(KJ)= ZA(KJ-1)*TA(KJ)
      ZA(KJ)= PB(KJ)*(ZA(KJ-1)+SAA(KJ))/(PB(KJ)+SAB(KJ))
      240 CONTINUE
      ZE= ZA(NUM)
      IF (GZZ .LT. 0.) GO TO 634
      SE= CMLX(0.0,CS*GZ/RR)
      RGI= (SE-ZE)/(SE+ZE)
      GO TO 600
      245 GO TO 600
      634 GYCS= -CS*GYZ/RR
      RGI= (GYCS-ZE)/(GYCS+ZE)
      C*****
      C COMPUTATION OF THE CONTRIBUTION FROM ONE SEGMENT
      C*****
      250 A= B*G
      WEX= W(I)*EX
      IF (TEE.NE.0) GO TO 650
      C*****CALL FUNCTION J0X *****
      255 J=RF1*J0X(A)*G3/GK
      GO TO 801
      650 IF (TEE .NE. 1) GO TO 700
      C*****CALL FUNCTION J0X *****
      J=RF1*J0X(A)*G*GK
      GO TO 801
      260 IF (TEE .NE. 2) GO TO 750
      C*****CALL FUNCTION J0X *****
      J=RF1*J0X(A)*G*RR/GK
      GO TO 801
      265 IF (TEE .NE. 3) GO TO 800
      C*****CALL FUNCTION J1X *****
      J= J1X(A)*G2*RF1
      GO TO 801
      270 IF (TEE .NE. 4) GO TO 850
      C*****CALL FUNCTION J1X *****
      J= RR*RG1*J1X(A)/GK
      GO TO 801
      C*****CALL FUNCTION J1X *****
      850 J= GK*J1X(A)*RF1
      275 JWEX= J*WEX
      RD= REAL(JWEX)
      RI= AIMAG(JWEX)
      SUMR= SUMR+RD
      SUMI= SUMI+RI
      280 CONTINUE
      C*****
      C VALUE OF ONE SEGMENT ROUNDED BY TWO CONSECUTIVE ZEROS OF J0 OR J1
      C*****
      285 AREAR(L)=MUJ*SUMR
      AREAL(L)=MUJ*SUMI

```

```

IF (L.GE.3) GO TO 1100
EPS=1.E-08
ER= ABS (AREAR(1))*EPS
EI= ABS (AREAI(1))*EPS
TR2= ABS (AREAR(L))
TI2= ABS (AREAI(L))
290 CONTINUE
950 CONTINUE
L=L+1
GO TO 90
1100 TRI=TR2
TII=TI2
TR2= ABS (AREAR(L))
TI2= ABS (AREAI(L))
R00L=(TR2.GT.TRI).OR.(TI2.GT.TII)
IF (.NOT.(R00L.AND.(L.EQ.N))) GO TO 1200
L=N
GO TO 2000
1200 IF (R00L) GO TO 950
R00L=(TR2.GE.FR).OR.(TI2.GE.EI)
IF (.NOT.(R00L.AND.(L.EQ.N))) GO TO 1300
L=1000000
GO TO 2000
1300 IF (R00L) GO TO 950
SUR=0.
SUI=0.
DO 1400 I=1,L
SUR=SUR+AREAR(I)
SUI=SUI+AREAI(I)
1400 CONTINUE
TREAL=SUR
TIMAG=SUI
C ***** RETURN *****
RETURN
2000 CONTINUE
C ***** CALL SUBROUTINE EULER *****
CALL EULER (N/2,N,ARFAR,EIJSUR)
C ***** CALL SUBROUTINE EULER *****
CALL EULER (N/2,N,ARFAI,EIJSUI)
SUR=0.
SUI=0.
N2I=N/2-1
DO 2200 I=1,N2I
SUR=SUR+AREAR(I)
SUI=SUI+AREAI(I)
2200 CONTINUE
SUR=SUR+EUSUR
SUI=SUI+EUSUI
WRITE (6,699) TEE,EIJSUR,EUSUI,SUR,SUI
699 FORMAT (2X,I2,2X,4E15.8)
TREAL=SUR
TIMAG=SUI
C ***** RETURN *****
RETURN
END

```

```

1 SUBROUTINE EULER (M,N,Z,SUM)
C *****
C THIS SUBROUTINE FINDS THE EULER'S SUMMATION WHEN THE INTEGRAL DUEFS
C NOT CONVERGE AFTER 44 SEGMENTS.
C IT IS CALLED FROM THE SUBROUTINE SUBM TWICE AFTER STATEMENT NUMBER 2000.
C *****
REAL Z(45),B(100),SUM,FAC
C ***** RETURN *****
IF (M.GT.N.OR.M.LE.0) RETURN
10 K = N-M+1
L = M-1
SUM = 0.
DO 10 I=1,K,2
10 B(I) = Z(L+I)
DO 20 I=2,K,2
20 B(I) = -Z(L+I)
KP=K+1
DO 40 I=2,K
KM=KP-I
DO 30 J=1,KM
KI=KP-J
30 B(KI) = -B(KI-1) + B(KI)
40 CONTINUE
FAC = .5
25 DO 50 I=1,K
SUM = SUM + FAC*B(I)
FAC = .5*FAC
50 ***** RETURN *****
C ***** RETURN *****
RETURN
END
30

```

```

1 REAL FUNCTION JOX(X)
C *****
C THIS SUBROUTINE COMPUTES THE BESSEL FUNCTION J0.
C IT IS CALLED FROM THE SUBROUTINE SUBM AFTER STATEMENT NUMBERS
5 C 600,650 AND 700.
REAL X,I,Y,F0,PHO
C *****
C TEST FOR THE TWO DIFFERENT PATHS THAT MAY BE FOLLOWED.
C *****
IF (X.GT.3.) GO TO 10
T=X/3.
Y=I*T
15 JOX = 1.-Y*(2.2499997-Y*(1.2656208-Y*(.3163866-Y*(.0444479-Y*
(3.9444E-3-2.*F-4*Y))))))
RETURN
10 Y=3./X
F0 = .79788456-Y*(7.7E-7+Y*(.55274E-2+Y*(.9512E-4-Y*
(.137237E-3-Y*(.72805F-3-.14476F-3*Y))))))
20 PHO = .7853981+Y*(.04166397+Y*(.3954E-4-Y*(.00262573-Y*
(.54125E-3+Y*(.29333F-3+.13558E-3*Y))))))
JOX = SQR(T1./X)*F0* COS(X-PHO)
***** RETURN *****
RETURN
END
25

```

```

1 REAL FUNCTION JIX(X)
C*****
C THIS SUBROUTINE COMPUTES THE BESSEL FUNCTION J1.
C IT IS CALLED FROM THE SUBROUTINE SUBM AFTER STATEMENT NUMBERS
C 750,800 AND 850.
C*****
REAL X,Y,I,FI,PHI
C*****
C TEST FOR THE TWO DIFFERENT PATHS THAT MAY BE FOLLOWED.
C*****
10 IF (X.GT.3.) GO TO 10
T = X/3.
Y = T*T
JIX = X*(.5-Y*(.5624985-Y*(.21093573-Y*(.03954289-Y*
1 (.00443319-Y*(.31761F-3-.1109E-4*Y))))))
C***** RETURN *****
RETURN
10 Y = 3./X
FI = .79788456+Y*(.156E-5+Y*(.01659667+Y*(.17105E-3-Y*
20 (.00249511-Y*(.00113653-.20033E-3*Y))))
PHI = .78539816-Y*(.12499612+Y*(.5650E-4-Y*(.00637879-Y*
1 (.74348E-3+Y*(.79824E-3-.29166E-3*Y))))
JIX = SQRT(1./X)*FI* SIN(X-PHI)
C***** RETURN *****
RETURN
25 END

```

```

1 FUNCTION GG (X,GU,GL)
C*****
C THIS SUBROUTINE CALCULATES THE VARIABLE G FOR USE IN GAUSSIAN QUADRATURE.
C IT IS CALLED FROM THE SUBROUTINE CALC 2 LINES AFTER STATEMENT NUMBER 98.
C*****
REAL X,GU,GL
GG = .5*(X*(GU-GL)+GL+GU)
C***** RETURN *****
RETURN
10 END

```

E.M. DIPOLE SOUNDING RESULTS OVER PERMAFROST

NO. OF LAYERS, COIL SEP., SIGMA1, AND SIGM/SIG1 VALUES FROM BOTTOM UPWARDS

2 3.000 .001 100.000 1.000
 THICKNESSES OF LAYERS IN METERS FROM BOTTOM UPWARDS

0.00 15.00
 DIELECTRIC CONSTANTS OF THE LAYERS FROM BOTTOM UPWARDS

B	RA1	AIM1	RA2	AIM2	RA3	AIM3	RA4	AIM4	RA5	AIM5
.005960	.364514E+02	.102504E+03	.136376E+01	.143746E+02	.182424E+02	.535398E+02	.910277E+01	.244819E+02	.303694E+02	.846570E+02
.008427	.757958E+02	.168528E+03	.352625E+01	.273263E+02	.379479E+02	.888226E+02	.189171E+02	.398526E+02	.631419E+02	.138921E+03
.013318	.178038E+03	.299698E+03	.108383E+02	.618478E+02	.891958E+02	.161138E+03	.443775E+02	.692788E+02	.148277E+03	.245984E+03
.018818	.307449E+03	.436167E+03	.224637E+02	.112161E+03	.154089E+03	.240412E+03	.765046E+02	.978741E+02	.255969E+03	.356027E+03
.026568	.483313E+03	.614154E+03	.412730E+02	.201552E+03	.242102E+03	.351121E+03	.119896E+03	.131504E+03	.402139E+03	.497105E+03
.032485	.602398E+03	.750108E+03	.553814E+02	.284607E+03	.301243E+03	.440557E+03	.148952E+03	.154748E+03	.500900E+03	.603237E+03
.041799	.759699E+03	.984030E+03	.745657E+02	.443444E+03	.377733E+03	.599922E+03	.186510E+03	.192002E+03	.630807E+03	.784023E+03
.049292	.862087E+03	.120169E+04	.860449E+02	.598345E+03	.425057E+03	.751234E+03	.209616E+03	.225125E+03	.714471E+03	.951213E+03
.058621	.963832E+03	.152040E+04	.940824E+02	.828035E+03	.467448E+03	.974076E+03	.230237E+03	.273120E+03	.796052E+03	.119569E+04
.081532	.111803E+04	.258194E+04	.732378E+02	.158893E+04	.488909E+03	.171592E+04	.241544E+03	.433350E+03	.906412E+03	.201024E+04
.098210	.115176E+04	.365998E+04	.207202E+01	.235111E+04	.408414E+03	.246776E+04	.206051E+03	.598905E+03	.905258E+03	.283940E+04
.111538	.112032E+04	.475646E+04	.110516E+03	.311711E+04	.256299E+03	.323091E+04	.140325E+03	.771604E+03	.840496E+03	.368449E+04
.132182	.101072E+04	.701502E+04	.450388E+03	.466529E+04	.991756E+01	.509465E+04	.795027E+02	.113775E+04	.620774E+03	.5436226E+04
.147751	.572576E+03	.929061E+04	.937813E+03	.624262E+04	.858375E+03	.644335E+04	.393015E+03	.154770E+04	.119176E+03	.722818E+04
.159994	.118620E+03	.117467E+05	.157024E+04	.785870E+04	.179271E+04	.824220E+04	.771219E+03	.199468E+04	.436767E+03	.916630E+04
B-SQR	PH1	AMP1	PH2	AMP2	PH3	AMP3	PH4	AMP4	PH5	AMP5
.000036	.704241E+02	.108792E+03	.845804E+02	.144392E+02	.711846E+02	.565623E+02	.696040E+02	.261194E+02	.702653E+02	.899395E+02
.000071	.657841E+02	.184788E+03	.826470E+02	.275528E+02	.668662E+02	.965893E+02	.646074E+02	.441145E+02	.655573E+02	.152597E+03
.000177	.592872E+02	.348592E+03	.800603E+02	.627902E+02	.610339E+02	.184178E+03	.573578E+02	.822734E+02	.589188E+02	.287218E+03
.000354	.548204E+02	.533635E+03	.786746E+02	.114388E+03	.573427E+02	.285554E+03	.519866E+02	.124227E+03	.542854E+02	.438492E+03
.000706	.517987E+02	.781522E+03	.784272E+02	.205734E+03	.554133E+02	.426496E+03	.469437E+02	.177955E+03	.510284E+02	.639398E+03
.001055	.512327E+02	.962052E+03	.789885E+02	.289946E+02	.556366E+02	.533702E+03	.460934E+02	.214787E+03	.502954E+02	.784089E+03
.001747	.523308E+02	.124316E+04	.804549E+02	.449669E+03	.578040E+02	.708935E+03	.458313E+02	.267676E+03	.511806E+02	.100628E+04
.002430	.543445E+02	.147894E+04	.818167E+02	.604501E+03	.604983E+02	.863149E+03	.470431E+02	.307604E+03	.530892E+02	.118965E+04
.003436	.576281E+02	.180017E+04	.835178E+02	.833363E+03	.643642E+02	.108043E+04	.498695E+02	.357211E+03	.563456E+02	.143644E+04
.006648	.665964E+02	.281361E+04	.873610E+02	.159062E+02	.740964E+04	.608653E+02	.608653E+02	.496121E+03	.657295E+02	.220514E+04
.009645	.725317E+02	.383697E+04	.899495E+02	.235111E+04	.806074E+02	.250133E+04	.710144E+02	.633359E+03	.723166E+02	.298021E+04
.012441	.767415E+02	.488844E+04	.920305E+02	.311907E+04	.854644E+02	.324106E+04	.796928E+02	.784260E+03	.771497E+02	.377914E+04
.017472	.818013E+02	.708746E+04	.955143E+02	.468698E+04	.901115E+02	.509466E+04	.939972E+02	.114052E+04	.834855E+02	.547159E+04
.021830	.864733E+02	.930824E+04	.985435E+02	.631267E+04	.975882E+02	.650028E+04	.104248E+03	.159682E+04	.890554E+02	.722917E+04
.025598	.894214E+02	.117473E+05	.101299E+03	.801404E+04	.102271E+03	.843491E+04	.111138E+03	.213858E+04	.927280E+02	.917670E+04

E.M. DIPOLE SOUNDING RESULTS OVER PERMAFROST

NO. OF LAYERS, COIL SEP., SIGMA1, AND SIGM/SIG1 VALUES FROM BOTTOM UPWARDS

2	10.000	.001	100.000	1.000
THICKNESSES OF LAYERS IN METERS FROM BOTTOM UPWARDS				

0.00	15.00
DIELECTRIC CONSTANTS OF THE LAYERS FROM BOTTOM UPWARDS	

B	20.00		6.00		AIM1		RA2		AIM2		RA3		AIM3		RA4		AIM4		RA5		AIM5	
	RA1	AIM1	RA2	AIM2	RA3	AIM3	RA4	AIM4	RA5	AIM5	PH1	PH2	PH3	PH4	PH5	AMP1	AMP2	AMP3	AMP4	AMP5		
.019866	.132298E+04	.320380E+04	.165081E+03	.899124E+03	.668885E+03	.173136E+04	.327024E+03	.736217E+03	.116000E+04	.262668E+04												
.028090	.272414E+04	.508218E+04	.424007E+03	.162516E+04	.138474E+04	.279239E+04	.669603E+03	.114459E+04	.226250E+04	.415119E+04												
.044392	.627474E+04	.835682E+04	.128692E+04	.328514E+04	.322420E+04	.476552E+04	.152464E+04	.179562E+04	.519959E+04	.676029E+04												
.062727	.106117E+05	.110278E+05	.263501E+04	.520777E+04	.551596E+04	.659009E+04	.254531E+04	.221873E+04	.877136E+04	.863102E+04												
.088562	.162572E+05	.133612E+05	.478545E+04	.778765E+04	.857126E+04	.859073E+04	.383235E+04	.238149E+04	.133931E+05	.104952E+05												
.108284	.199343E+05	.144815E+05	.640212E+04	.968556E+04	.106042E+05	.990548E+04	.464105E+04	.228709E+04	.163837E+05	.111791E+05												
.139329	.246540E+05	.157768E+05	.869909E+04	.127438E+05	.132517E+05	.119263E+05	.563306E+04	.192344E+04	.201923E+05	.118003E+05												
.164307	.276872E+05	.167464E+05	.102804E+05	.154289E+05	.149573E+05	.137135E+05	.623342E+04	.151805E+04	.226146E+05	.124765E+05												
.195404	.308201E+05	.181470E+05	.119281E+05	.192274E+05	.165571E+05	.163225E+05	.678778E+04	.917959E+03	.250739E+05	.127102E+05												
.271775	.365672E+05	.232178E+05	.147064E+05	.315563E+05	.193731E+05	.250435E+05	.749326E+04	.890568E+03	.293823E+05	.146834E+05												
.402120E+05	.288288E+05	.157614E+05	.440287E+05	.202409E+05	.341100E+05	.753301E+04	.753301E+04	.248934E+04	.318494E+05	.175518E+05												
.371794	.436500E+05	.350700E+05	.160130E+05	.567828E+05	.195727E+05	.437756E+05	.711178E+04	.397730E+04	.338729E+05	.207070E+05												
.440608	.499978E+05	.480823E+05	.151192E+05	.833621E+05	.185754E+05	.637836E+05	.540943E+04	.640901E+04	.369865E+05	.277074E+05												
.492502	.586717E+05	.632021E+05	.130524E+05	.111790E+06	.143855E+05	.908778E+05	.334016E+04	.825389E+04	.413771E+05	.364668E+05												
.533312	.693880E+05	.798585E+05	.103369E+05	.142658E+06	.131499E+05	.113605E+06	.864025E+03	.624542E+04	.468205E+05	.486873E+05												
B-SQR	PH1	AMP1	PH2	AMP2	PH3	AMP3	PH4	AMP4	PH5	AMP5												
.000395	.675623E+02	.346621E+04	.795962E+02	.914153E+03	.688768E+02	.185608E+04	.660494E+02	.805581E+03	.672776E+02	.284771E+04												
.000789	.618079E+02	.576624E+04	.753774E+02	.167956E+04	.636282E+02	.311742E+04	.596716E+02	.132007E+04	.614086E+02	.472771E+04												
.001971	.530988E+02	.104503E+05	.686077E+02	.352821E+04	.559190E+02	.575375E+04	.496656E+02	.235558E+04	.524675E+02	.853496E+04												
.003935	.461015E+02	.153043E+05	.631617E+02	.583645E+04	.500704E+02	.859390E+04	.410705E+02	.337659E+04	.451942E+02	.124468E+05												
.007843	.394156E+02	.210433E+05	.584296E+02	.914047E+04	.450866E+02	.121400E+05	.318575E+02	.451203E+04	.380832E+02	.170154E+05												
.011726	.359970E+02	.246392E+05	.565354E+02	.116102E+05	.430487E+02	.145110E+05	.262339E+02	.517398E+04	.43071E+02	.198343E+05												
.019413	.326164E+02	.292699E+05	.556819E+02	.154298E+05	.419867E+02	.178282E+05	.188505E+02	.595309E+04	.303019E+02	.233875E+05												
.026997	.311673E+02	.323577E+05	.563242E+02	.185402E+05	.425159E+02	.202924E+05	.136870E+02	.641561E+04	.282995E+02	.256844E+05												
.038183	.304898E+02	.357658E+05	.581858E+02	.226268E+05	.445955E+02	.232517E+05	.770176E+01	.684959E+04	.268809E+02	.281114E+05												
.073862	.324129E+02	.433154E+05	.650128E+02	.348150E+05	.522719E+02	.316593E+05	.677777E+01	.754536E+04	.268641E+02	.329363E+05												
.107168	.356375E+02	.494783E+05	.703037E+02	.467648E+05	.593150E+02	.396663E+05	.182865E+02	.795366E+04	.288586E+02	.363655E+05												
.138231	.387979E+02	.559931E+05	.742513E+02	.589975E+05	.659099E+02	.479520E+05	.292163E+02	.814840E+04	.314381E+02	.397108E+05												
.194135	.438812E+02	.693664E+05	.797201E+02	.847220E+05	.737631E+02	.664333E+05	.498345E+02	.836673E+04	.368377E+02	.462137E+05												
.242258	.471289E+02	.862373E+05	.833404E+02	.112550E+06	.810050E+02	.920094E+05	.679679E+02	.890412E+04	.443906E+02	.551533E+05												
.284422	.490127E+02	.105793E+06	.858557E+02	.143032E+06	.833973E+02	.114363E+06	.821234E+02	.630490E+04	.462371E+02	.676914E+05												

E.M. DIPOLE SOUNDING RESULTS OVER PERMAFROST

NO. OF LAYERS, COIL SEP., SIGMA1 AND SIGM/SIG1 VALUES FROM BOTTOM UPWARDS

3	3.000	.020	.500	.025	1.000
---	-------	------	------	------	-------

THICKNESSES OF LAYERS IN METERS FROM BOTTOM UPWARDS

0.00	20.00	1.00
------	-------	------

DIELECTRIC CONSTANTS OF THE LAYERS FROM BOTTOM UPWARDS

B	RA1	AIM1	RA2	AIM2	RA3	AIM3	RA4	AIM4	RA5	AIM5
.026657	.206851E+01	.962247E+02	.433202E-01	.893057E+02	.103455E+01	.769092E+02	.515313E+00	.865770E+01	.172255E+01	.699216E+02
.037697	.503335E+01	.190448E+03	.141930E+00	.178583E+03	.251773E+01	.156817E+03	.125111E+01	.168151E+02	.418964E+01	.138175E+03
.059599	.154862E+02	.467822E+03	.665423E+00	.446287E+03	.774829E+01	.387893E+03	.382670E+01	.399635E+02	.128753E+02	.338523E+03
.084274	.348693E+02	.920920E+03	.212367E+01	.892157E+03	.174531E+02	.768418E+03	.853941E+01	.762473E+02	.289392E+02	.664778E+03
.119149	.768944E+02	.181031E+04	.683503E+01	.178313E+04	.384923E+02	.152104E+04	.165150E+02	.144610E+03	.636062E+02	.130328E+04
.145886	.122412E+03	.268760E+04	.136994E+02	.267342E+04	.612515E+02	.226276E+04	.290068E+02	.209946E+03	.100946E+03	.193170E+04
.188234	.224721E+03	.442233E+04	.335288E+02	.445256E+04	.112382E+04	.375057E+04	.518294E+02	.335694E+03	.184367E+03	.317202E+04
.222597	.344038E+03	.614054E+04	.613010E+02	.623029E+04	.171977E+03	.522534E+04	.773622E+02	.457143E+03	.280935E+03	.439846E+04
.265833	.552734E+03	.869668E+04	.117677E+03	.889479E+04	.278788E+03	.742265E+04	.121552E+03	.634309E+03	.452594E+03	.622048E+04
.374900	.158240E+04	.170790E+05	.431752E+03	.177599E+05	.788342E+03	.146910E+05	.324094E+03	.118736E+04	.127103E+04	.121777E+05
.457881	.308011E+04	.252585E+05	.936519E+03	.265972E+05	.152708E+04	.218483E+05	.607940E+03	.168682E+04	.245885E+04	.179663E+05
.527247	.501174E+04	.332211E+05	.162658E+04	.354013E+05	.247379E+04	.288897E+05	.964175E+03	.212949E+04	.398438E+04	.235679E+05
.642163	.101100E+05	.484691E+05	.353890E+04	.528923E+05	.489362E+04	.427282E+05	.184216E+04	.262955E+04	.796996E+04	.342038E+05
.737395	.163295E+05	.626918E+05	.612290E+04	.702073E+05	.799425E+04	.558851E+05	.208632E+04	.328493E+04	.128157E+05	.439898E+05
.819865	.237507E+05	.760353E+05	.933874E+04	.873335E+05	.115107E+05	.686040E+05	.404550E+04	.350000E+04	.185420E+05	.536321E+05
B-SQR	PH1	AMP1	PH2	AMP2	PH3	AMP3	PH4	AMP4	PH5	AMP5
.000711	.887685E+02	.962469E+02	.899722E+02	.893057E+02	.892489E+02	.769160E+02	.865937E+02	.867302E+01	.885888E+02	.699428E+02
.001421	.884861E+02	.190514E+03	.899545E+02	.178583E+03	.890022E+02	.156838E+03	.857448E+02	.168615E+02	.882633E+02	.136239E+03
.003552	.881040E+02	.468076E+03	.899146E+02	.446286E+03	.888557E+02	.387971E+03	.845303E+02	.401463E+02	.878219E+02	.336768E+03
.007102	.878316E+02	.921580E+03	.898636E+02	.892159E+03	.886990E+02	.768616E+03	.836097E+02	.767240E+02	.875074E+02	.665498E+03
.014196	.875678E+02	.181194E+04	.897804E+02	.178315E+04	.885504E+02	.152153E+04	.821039E+02	.145791E+03	.872059E+02	.130433E+04
.021283	.873921E+02	.269038E+04	.897064E+02	.267345E+04	.884527E+02	.226842E+04	.821337E+02	.211941E+03	.870086E+02	.193433E+04
.035432	.870910E+02	.442804E+04	.895686E+02	.445268E+04	.882837E+02	.375225E+04	.812231E+02	.339672E+03	.866735E+02	.317737E+04
.049549	.867932E+02	.615017E+04	.894363E+02	.623059E+04	.881150E+02	.522817E+04	.803949E+02	.463642E+03	.863454E+02	.440743E+04
.070667	.863338E+02	.871452E+05	.892420E+02	.889556E+04	.878503E+02	.743178E+04	.791383E+02	.645575E+03	.858386E+02	.623692E+04
.140550	.847065E+02	.171521E+05	.8868074E+02	.177652E+05	.869284E+02	.147121E+05	.747328E+02	.123079E+04	.840414E+02	.122438E+05
.209655	.830475E+02	.254456E+05	.879834E+02	.266137E+05	.860318E+02	.219016E+05	.701805E+02	.179383E+04	.822060E+02	.181314E+05
.277990	.814210E+02	.335970E+05	.873693E+02	.354386E+05	.851018E+02	.289956E+05	.656402E+02	.233759E+04	.804044E+02	.239024E+05
.412373	.782178E+02	.495123E+05	.861722E+02	.530105E+05	.834654E+02	.430078E+05	.569341E+02	.337638E+04	.768826E+02	.351181E+05
.543751	.754005E+02	.647836E+05	.850157E+02	.704738E+05	.818544E+02	.564280E+05	.486957E+02	.437282E+04	.737574E+02	.458186E+05
.672178	.726531E+02	.796584E+05	.838964E+02	.878314E+05	.804754E+02	.695563E+05	.408650E+02	.534940E+04	.707284E+02	.561802E+05

E.M. DIPOLE SOUNDING RESULTS OVER PFCMAFFPOST

NO. OF LAYERS, COIL SEP., SIGMA1 AND SIGMA2 STG1 VALUES FROM BOTTOM UPWARDS

3 10.000 .020 .500 .02F 1.000
 THICKNESSES OF LAYERS IN METERS FROM BOTTOM UPWARDS

0.00 20.00 1.00
 DIELECTRIC CONSTANTS OF THE LAYERS FROM BOTTOM UPWARDS

R	25.00	RA1	AIM1	6.00	RA2	20.00	AIM2	RA3	AIM3	RAL	AIM4	PA5	AIM5
.08855	.755966F+02	.600623F+03	.447842E+01	.798399F+03	.390206E+02	.784697E+03	.187675F+02	.920375F+02	.629082F+02	.339057F+03			
.125657	.182507F+03	.112732F+04	.140470E+02	.159324E+04	.921015F+02	.153237E+04	.451122F+02	.202530F+03	.151746F+03	.616525E+03			
.199664	.550584F+03	.251264F+04	.604863E+02	.396220E+04	.240172E+03	.367763E+04	.134628E+03	.582517E+03	.456808E+03	.128675E+04			
.280914	.120462E+04	.443558F+04	.175787E+03	.78733E+04	.620411F+03	.708392E+04	.28978E+03	.129222E+04	.996254E+03	.212823E+04			
.3971F3	.252143E+04	.782398E+04	.499675E+03	.156034E+05	.132703E+04	.135879E+05	.897502E+03	.288258E+04	.207263E+04	.329423E+04			
.486247	.382444E+04	.107319E+05	.919147E+03	.232500E+05	.205433E+04	.198719E+05	.863078E+03	.457138E+04	.312503E+04	.410686E+04			
.627445	.643757E+04	.158570E+05	.200286E+04	.383763E+05	.358957E+04	.320808E+05	.136179E+04	.811607E+04	.519967E+04	.516000E+04			
.741930	.913653E+04	.204185E+05	.339156E+04	.533415E+05	.526641E+04	.439947E+05	.181161E+04	.117931F+05	.720899F+04	.574957E+04			
.885108	.135064E+05	.265912E+05	.602846E+04	.755564E+05	.815577E+04	.615629E+05	.242026E+04	.174713E+05	.106184E+05	.607414E+04			
1.249666	.310019E+05	.429177E+05	.194892E+05	.147861E+06	.206590E+05	.117427E+06	.408064E+04	.373253E+05	.233913E+05	.366843E+04			
1.526271	.531322F+05	.534649F+05	.398059E+05	.217431E+06	.377195E+05	.169992E+06	.516572E+04	.583305F+05	.389692E+05	.339833E+04			
1.757491	.791754E+05	.585624E+05	.664531E+05	.283801E+06	.584524E+05	.219287E+06	.536074E+04	.803695E+05	.567508E+05	.149167E+05			
2.140542	.137171E+06	.515207E+05	.136474E+06	.405596E+05	.109921E+06	.307147E+06	.227972E+04	.126789E+06	.928205F+05	.515182E+05			
2.457983	.199304E+06	.242457E+05	.225395E+06	.511291E+06	.168917E+06	.382529E+06	.624501E+04	.175081E+06	.128024F+06	.103815E+06			
2.732882	.259536E+06	.218985E+05	.329637E+06	.599839E+06	.235962F+06	.444794E+06	.217901F+05	.223131E+06	.156431E+06	.169734E+06			
B-SRR	PH1	AMPI	P42	AMP2	PH3	AMP3	PH4	AMP4	PH5	AMP5			
.037895	.328263E+02	.605362E+03	.896786E+02	.798411E+03	.872260F+02	.785617E+03	.784759E+02	.939311E+02	.794889E+02	.344843E+03			
.015790	.908039E+02	.114200E+04	.894949E+02	.159331E+04	.865604E+02	.153514E+04	.774428E+02	.207494E+02	.761726F+02	.634925E+03			
.039467	.776404E+02	.257226F+04	.891254E+02	.396275F+04	.356435E+02	.368828E+04	.769866E+02	.597872E+03	.704547E+02	.136543E+04			
.079913	.749676E+02	.464451E+04	.887210E+02	.787539E+04	.849347E+02	.711094E+04	.774274E+02	.133114E+04	.648737E+02	.234635E+04			
.157738	.721374E+02	.822024F+04	.881658E+02	.156114E+05	.944221F+02	.135526E+05	.784803E+02	.294184E+04	.578232F+02	.389201E+04			
.236876	.703858E+02	.113929F+05	.877341E+02	.232682E+05	.840978E+02	.199777E+05	.793084E+02	.465214E+04	.527314E+02	.516063E+04			
.393688	.679040E+02	.171139E+05	.870124E+02	.384286E+05	.836156E+02	.322810E+05	.804711E+02	.822953E+04	.447806E+02	.732544E+04			
.5505F0	.656932E+02	.223694E+05	.863619E+02	.534493E+05	.831713E+02	.443090E+05	.812667E+02	.119314E+05	.782234E+02	.929093E+04			
.785188	.630719E+02	.298238E+05	.854382E+02	.757966E+05	.825450F+02	.628378E+05	.821131E+02	.176391E+05	.297713E+02	.123330E+05			
1.566185	.541573E+02	.529479E+05	.824926E+02	.149159E+06	.800225E+02	.119230E+06	.837609E+02	.375477E+05	.895111F+01	.236797E+05			
2.329503	.451788E+02	.753759E+05	.796255E+02	.221045E+06	.774897E+02	.174127E+06	.849391E+02	.585588F+05	.499666E+01	.390175E+05			
3.088776	.364886E+02	.984799E+05	.768214E+02	.291479E+06	.750745F+02	.226844E+06	.861840E+02	.805481F+05	.148268F+02	.582917E+05			
4.581919	.205859E+02	.146527E+06	.714031E+02	.427940E+06	.703085E+02	.326224E+06	.889699E+02	.126809E+06	.829316F+02	.106159E+06			
6.0541681	.693634E+01	.205774E+06	.682147E+02	.558749E+06	.661747F+02	.418164E+06	.920428E+02	.175192E+06	.390387E+02	.164826E+06			
7.468645	-.482295E+01	.260458E+06	.612054E+02	.684647E+06	.620541E+02	.503507E+06	.9555776E+02	.224193E+06	.473357E+02	.230825E+06			